



HAL
open science

**Zinc, aluminum and group 3 metal complexes of
sterically demanding naphthoxy-pyridine ligands:
Synthesis, structure, and use in ROP of racemic lactide
and β -butyrolactone**

Yulia Chapurina, Thierry Roisnel, Jean-François Carpentier, Evgeny Kirillov

► **To cite this version:**

Yulia Chapurina, Thierry Roisnel, Jean-François Carpentier, Evgeny Kirillov. Zinc, aluminum and group 3 metal complexes of sterically demanding naphthoxy-pyridine ligands: Synthesis, structure, and use in ROP of racemic lactide and β -butyrolactone. *Inorganica Chimica Acta Reviews*, 2015, 431, pp.161-175. 10.1016/j.ica.2014.11.002 . hal-01091458

HAL Id: hal-01091458

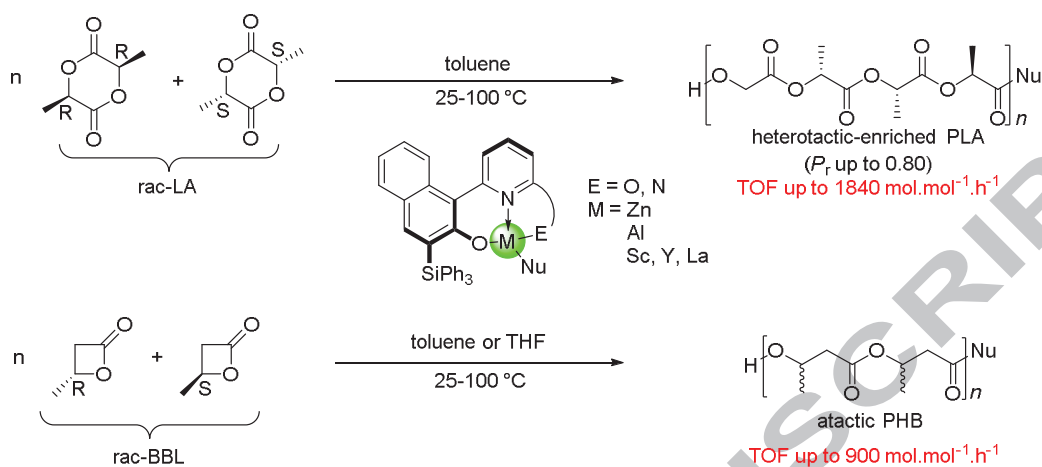
<https://univ-rennes.hal.science/hal-01091458>

Submitted on 5 Dec 2014

HAL is a multi-disciplinary open access archive for the deposit and dissemination of scientific research documents, whether they are published or not. The documents may come from teaching and research institutions in France or abroad, or from public or private research centers.

L'archive ouverte pluridisciplinaire **HAL**, est destinée au dépôt et à la diffusion de documents scientifiques de niveau recherche, publiés ou non, émanant des établissements d'enseignement et de recherche français ou étrangers, des laboratoires publics ou privés.

For the Table of content entry



Zinc, aluminum and group 3 metal complexes supported by tridentate naphthoxy-pyridine ligands were prepared and used as initiators/catalysts for the ring-opening polymerization of *racemic*-lactide and *racemic*-β-butyrolactone, affording heterotactic- enriched PLAs and atactic PHBs, respectively.

Zinc, Aluminum and Group 3 Metal Complexes of Sterically Demanding Naphthoxy-Pyridine Ligands: Synthesis, Structure, and Use in ROP of *racemic* Lactide and β -Butyrolactone

Yulia Chapurina,^a Thierry Roisnel,^b Jean-François Carpentier^{*a} and Evgeny Kirillov^{*a}

^a *Organometallics: Materials and Catalysis and* ^b *Centre de Diffractométrie X, Institut des Sciences Chimiques de Rennes, UMR 6226 CNRS-Université de Rennes 1, F-35042 Rennes Cedex, France*

Abstract: New potentially tridentate, bulky *ortho*-Ph₃Si-substituted naphthol-pyridine proligands **a–f** were synthesized and introduced onto zinc, aluminum and group 3 metal centers (M = Sc, Y, La) using straightforward one-step alkane or amine elimination protocols. The solid-state structures of these mononuclear zinc (**1a**, **1c**, **1d**, **2c** and **2e**) and aluminum (**3c**) complexes were determined by single-crystal X-ray diffraction studies, while the solution structures were established using ¹H, ¹³C{¹H} and ²⁹Si/²⁹Si{¹H} (when appropriate) NMR spectroscopy. For all complexes, only one species (isomer) of C₁ symmetry was observed by NMR spectroscopy in the broad temperature range. Most of these complexes are effective initiators for the ring-opening polymerization (ROP) of *racemic* lactide (*rac*-LA) at 25–100 °C, affording poly(lactides)s (PLAs) generally with unimodal dispersities and molecular weights in good agreement with calculated values. An yttrium complex (**4e**) proved the most active (TOF = 1840 mol(LA)·mol(Y)⁻¹·h⁻¹ at 25 °C) and yielded heterotactic-enriched PLAs (*P_r* up to 0.80) in toluene, while atactic PHBs are formed in the ROP of *racemic* β -butyrolactone (*rac*-BBL) under the same conditions.

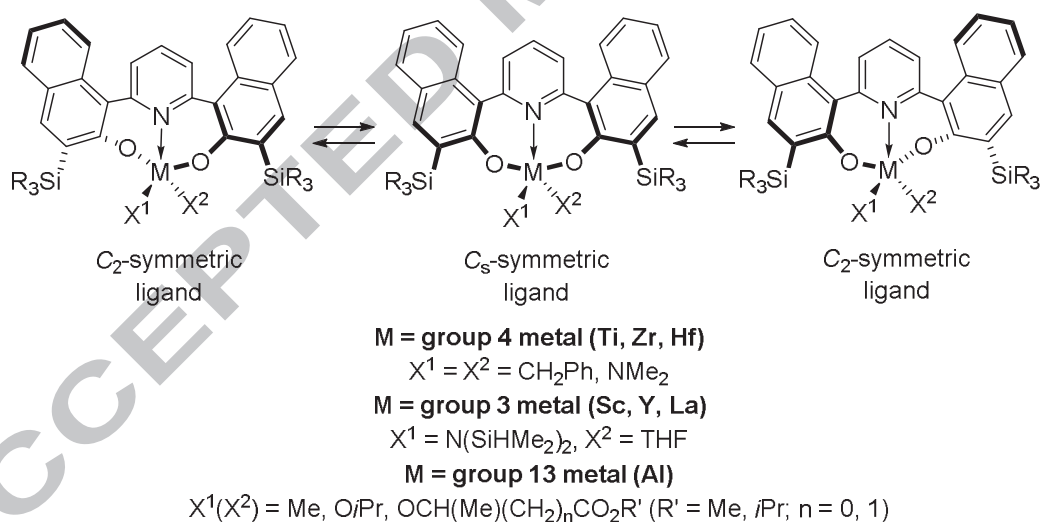
* Corresponding authors: Fax: (+33)(0)223-236-939. E-mail: evgueni.kirillov@univ-rennes1.fr; jean-francois.carpentier@univ-rennes1.fr

Introduction

Stereocontrolled ring-opening polymerization (ROP) of *racemic* cyclic esters (*e.g.*, lactide (*rac*-LA) and β -butyrolactone (*rac*-BBL)), mediated by discrete organometallic precursors, has been the subject of numerous studies in the last years.¹ Polymerization of these renewable monomers under appropriate conditions can lead to polymers exhibiting a wide range of microstructures (iso/hetero(syndio)/atactic, and also stereoblock and gradient), which may confer, in each specific case, high crystallinity, improved elastomeric properties and controlled biodegradability. The ligand nature (geometry) plays a pivotal role in the polymerization stereocontrol, even if stereoselection during coordination/insertion of the monomer onto a metal center occurs via a chain-end control (CEM) rather than an enantiomorphic site control mechanism (SCM), which is the more “natural” process for chirality transfer onto a growing polymeric chain.^{1,2}

In our ongoing survey of new ancillaries for engineering of potent catalysts/initiators for stereocontrolled ROP of cyclic esters, we have designed a bis(naphthoxy)pyridine ligand platform (Scheme 1).^{3,4} The non-coplanar orientation of the bridging pyridine and adjacent naphthoxy groups within the latter system, upon stereoselective coordination with group 4 metals (Ti, Zr and Hf), can give rise to two distinct geometries, namely, C_s -symmetric (*meso*-like) and C_2 -symmetric (*rac*-like) isomers.⁵ This interconversion between two geometries is anticipated to exert some special influence on the stereocontrollability of the metal complexes towards the polymerizations of cyclic esters such as *rac*-LA and *rac*-BBL, leading to polyesters with different tacticities (*e.g.*, atactic or hetero/syndiotactic). Also, if such interconversion would occur on the timescale of polymerization propagation (“oscillating” behavior), it could lead to stereoblock architectures (*i.e.*, macromolecules enchaining segments of different tacticities). In fact, reversible interconversion between such C_s - and C_2 -symmetric isomers of group 4 metal complexes has been demonstrated to take place in

toluene solution with a moderate activation barrier ($\Delta G^\ddagger_{298} = 13.8\text{--}15.6 \text{ kcal}\cdot\text{mol}^{-1}$). Yet, in our previous attempts intended to extend this coordination chemistry to groups 3 (Sc, Y and La) and 13 (Al) metals, for each compound, solely the isomer exhibiting the C_s -symmetric coordination of the ligand has been observed and isolated.⁵ For all of these different complexes, interconversion between the C_s - and a putative C_2 -symmetric isomers was not observed in solution using VT NMR spectroscopic studies. The latter behavior may stem either from a much higher interconversion barrier (kinetic control), intrinsic to such bis(naphthoxy)pyridine complexes of groups 3 and 13 metals, or from basic instability of the associated C_2 -isomer (thermodynamic control). When used as initiators/precatalysts in ROP of *rac*-LA and *rac*-BBL, these group 3 metal bis(naphthoxy)pyridine complexes were found to be moderately heteroselective and syndioselective, respectively, while the aluminum complexes appeared to be non-stereoselective.⁵

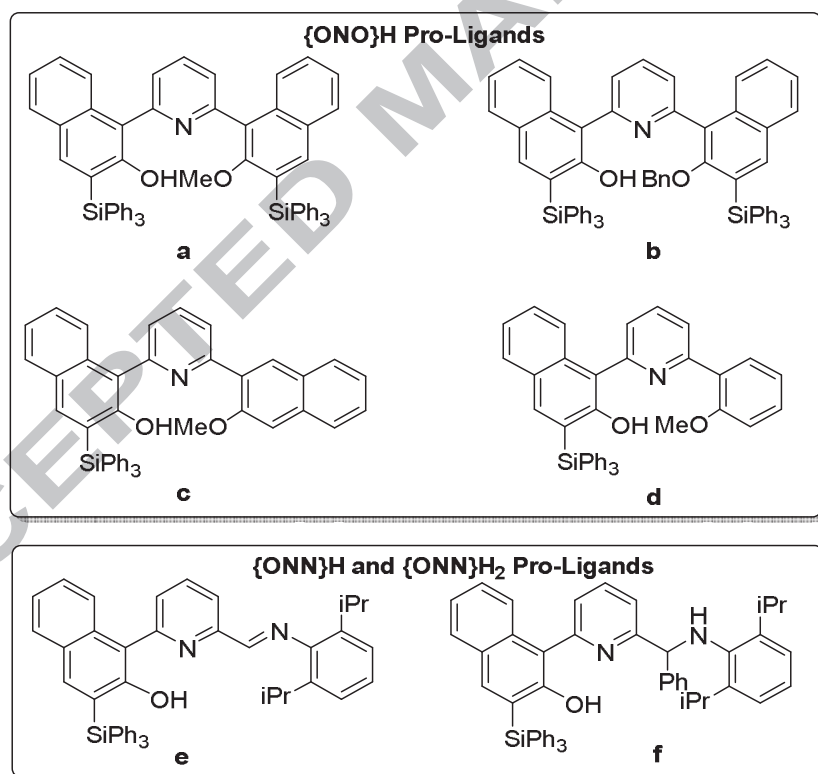


Scheme 1. Ph_3Si -substituted bis(naphthoxy)pyridine-based polymerization systems.

Thus, we decided to set up more flexible ligand platforms that combine the conformationally stable naphthoxy-pyridine scaffold and pending heteroatom-containing donating groups. We surmised that the implementation of these ligands would provide a less

sterically rigid binding with metal center⁶ and would allow preparation of complexes featuring relatively easy dynamic interconversion between isomers of different geometries.

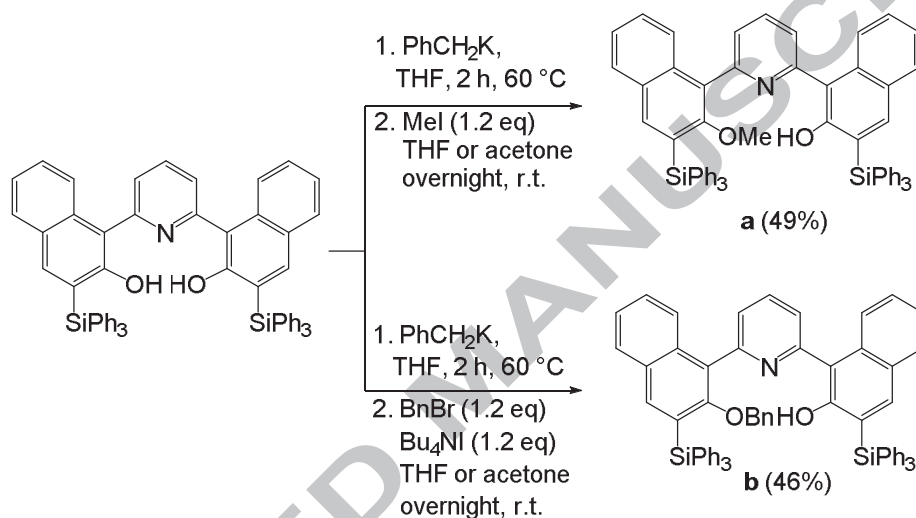
In this contribution, two main categories of asymmetrically substituted pyridine-naphthol proligands were considered (Scheme 2): (i) proligands **a–d** bearing *O*-based pendant donating groups, which would result in monoanionic $\{\text{ONO}\}^-$ ligand platforms, and (ii) proligands incorporating *N*-based pendant donating groups for the synthesis of complexes with both monoanionic $\{\text{ONN}\}^-$ (**e**) and dianionic $\{\text{ONN}\}^{2-}$ (**f**) ligand platforms. The synthesis of the corresponding complexes of zinc, aluminum and group 3 metals (Sc, Y and La) was investigated, and the obtained compounds were studied as initiators in the ROP of *rac*-LA and *rac*-BBL.



Scheme 2. Tridentate pyridine-linked naphthol-based proligands **a–f** used in this study.

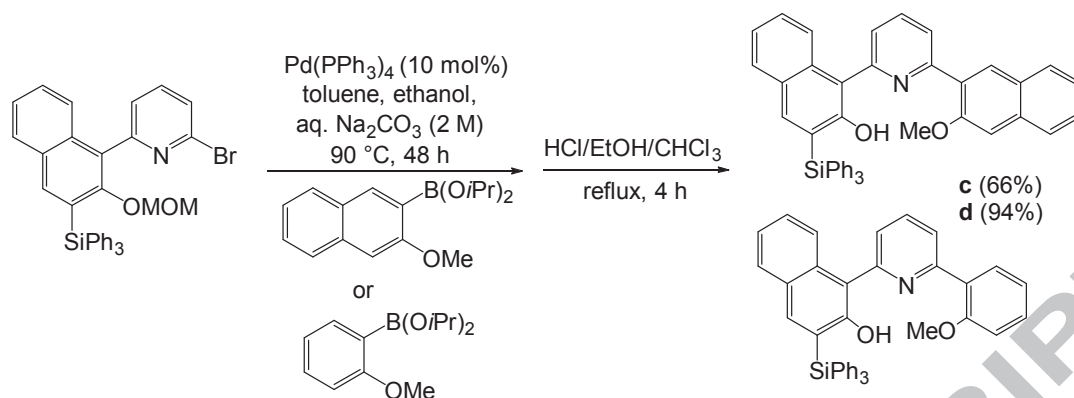
Results and Discussion

Synthesis of Proligands. Asymmetric pyridine-linked proligands **a** and **b** were prepared starting from the diproteo bis(naphthol)pyridine proligand previously described by our group (Scheme 3).^{5a} The two-step procedure involves deprotonation of the latter precursor with PhCH_2K in THF followed by methylation or benzylation reaction with MeI or BnBr/ Bu_4NI to afford **a** and **b**, respectively. Analytically pure proligands were obtained after column chromatography in 49% and 46% yields, respectively.



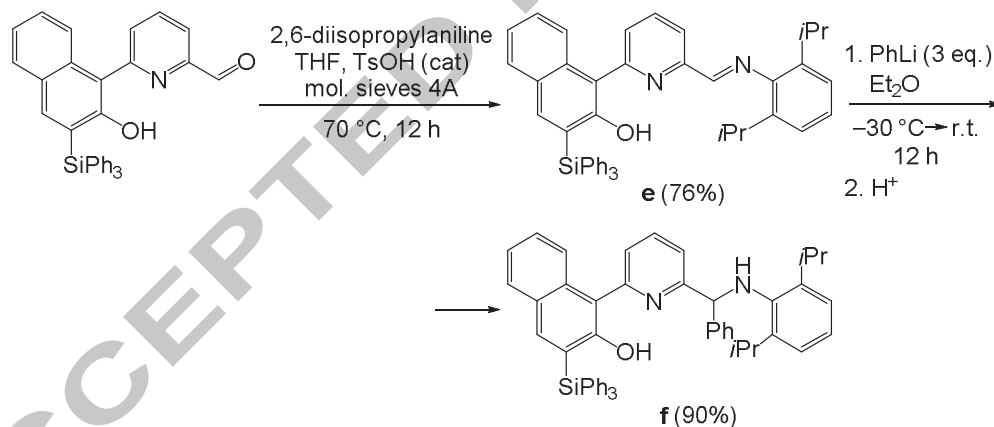
Scheme 3. Synthesis of proligands **a** and **b**.

The synthesis of **c** and **d** was accomplished via Suzuki coupling between 2-bromo-6-(2-(methoxymethoxy)-3-(triphenylsilyl)naphthalen-1-yl)pyridine (see the Experimental Section) and the corresponding boronic acid, followed by deprotection (Scheme 4). Both compounds were obtained in 66% and 94% yields, respectively, after recrystallization.



Scheme 4. Synthesis of proligands **c** and **d**.

Compound **e** was obtained in 76% yield by a standard condensation of 6-(2-hydroxy-3-(triphenylsilyl)naphthalen-1-yl)picolinaldehyde (see the Experimental Section) with 2,6-diisopropylaniline (Scheme 5). Further reaction of isolated **e** with a 3-fold excess of PhLi, followed by hydrolysis, gave compound **f** in 90% yield.



Scheme 5. Synthesis of proligands **e** and **f**.

Proligands **a–f** are stable compounds, readily soluble in aromatic hydrocarbons (benzene, toluene) and other common solvents (CHCl_3 , CH_2Cl_2 , THF). These compounds were fully characterized by ^1H and ^{13}C NMR spectroscopy, elemental analysis and X-ray crystallography (Figures S57 and Tables S1 and S2).

Synthesis of Zinc, Aluminum and Group 3 Metal Complexes. The preparation of alkyl- and amido-zinc complexes supported by these bulky naphthoxy-based ligands was carried out by direct σ -bond metathesis of ZnEt_2 and $\text{Zn}[\text{N}(\text{SiMe}_3)_2]_2$, respectively, with proligands **a–d**. Generally, the reactions took place in toluene at room temperature, concomitantly eliminating 1 equiv of ethane or $\text{HN}(\text{SiMe}_3)_2$, respectively.

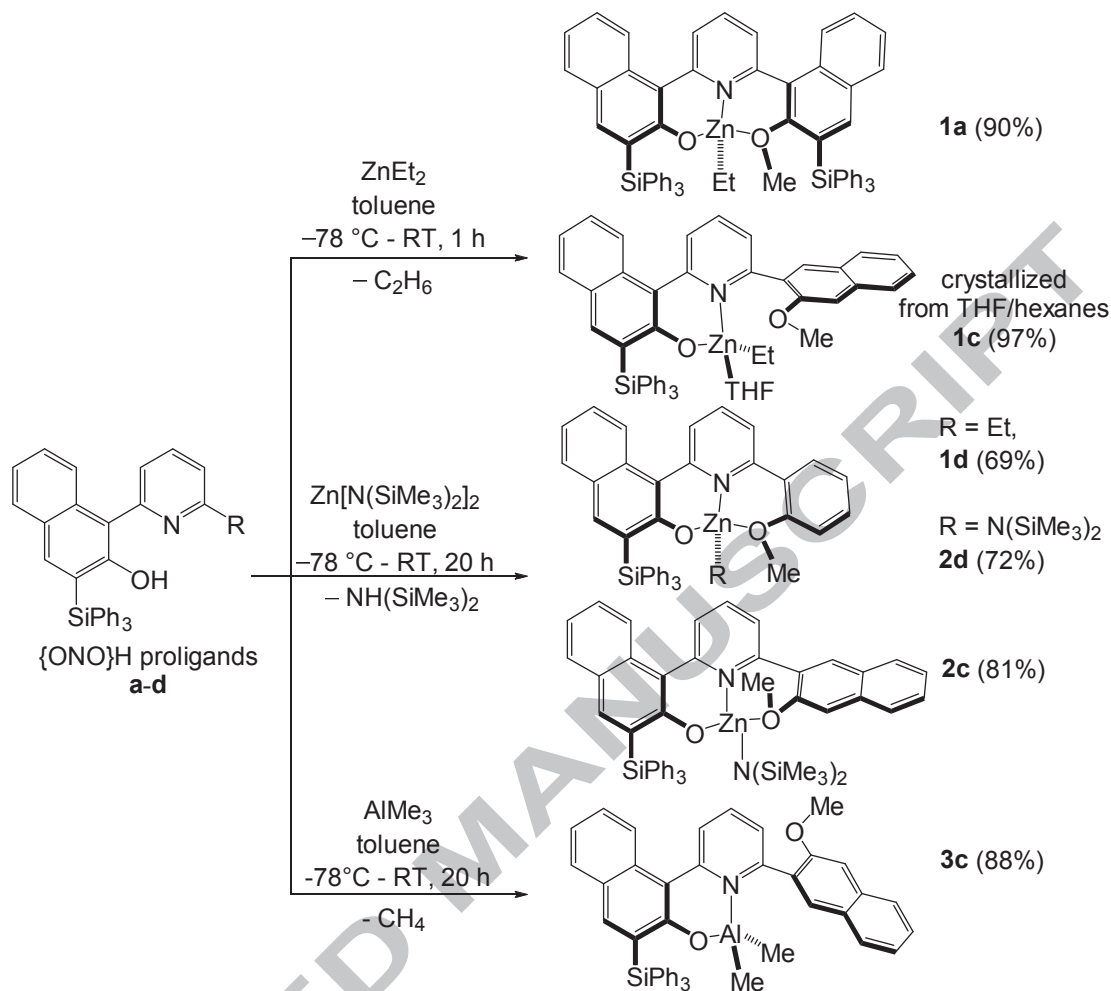
1. Ligands of ONO-type. Within the series of complexes of $\{\text{ONO}\}^-$ ligands (Scheme 2, top), both the corresponding ethyl-zinc (**1a**, **1c** and **1d**) and amido-zinc (**2c** and **2d**) compounds were isolated in high yields. The reaction of **b** with $\text{Zn}[\text{N}(\text{SiMe}_3)_2]_2$ appeared to be problematic, and mixtures of the desired complex **2b** with the initial proligand were systematically obtained. The outcome of these tests did not change even upon heating at 80 °C over one week. The reasons for such reactivity remained unclear, and **1b** was not isolated pure. The reaction of **b** with Et_2Zn did not take place in benzene or toluene even upon reflux.

In a similar manner, dimethyl-aluminum complex **3c** was prepared by treatment of the parent proligand with a small excess of AlMe_3 in toluene at room temperature and isolated as a red crystalline solid in 88% yield (Scheme 6). Due to difficulties encountered for Zn and Ln (*vide infra*) chemistries, neither **a** nor **b** were tested with Al.

The complexes were characterized by NMR spectroscopy in solution and elemental analysis and X-ray crystallography in the solid state (*vide infra*). The ^1H and $^{13}\text{C}\{^1\text{H}\}$ NMR spectra of **1a**, **1c**, **1d**, **2c**, **2d** and **3c** confirm the nature of the compounds. In particular, the ^{13}C NMR chemical shifts (less sensitive than ^1H signals to anisotropic effects quite likely in those complexes having multiple aromatic rings) for the $\text{Zn}-\text{CH}_2\text{CH}_3$ (δ -1.8 and 11.8 (**1a**), -1.2 and 12.8 (**1c**), -2.4 and 12.3 (**1d**) ppm), $\text{Zn}-\text{N}(\text{SiMe}_3)_2$ (δ 5.4 (**2c**), 5.5 (**2d**) and 4.9 (**2e**) ppm) and $\text{Al}-\text{Me}$ (δ -9.7 (**3c**) and -14.2 (**3e**) ppm) groups are in line with those reported in the literature for analogous Zn-ethyl,⁷ Zn-amido⁸ and Al-methyl^{4,5b,c} complexes. These NMR data also all testify of the asymmetric nature of these complexes in solution. Due to the substantial bulkiness of the ligand scaffolds, some of the complexes (**1a** and **1d**) exhibited a

moderate fluxional behavior. Hence, the room-temperature ^1H NMR spectrum of **1a** in toluene- d_8 (Figure S23) displayed a series of broadened signals due to fluxional dynamics arising from a hindered reorganization of the geometry (presumably, via reversible decoordination and rotation of the bulky MeO-naphthyl moiety and/or reciprocal reorganization of the adjacent naphthoxy and pyridine moieties). Upon lowering the temperature, all signals sharpened and a well-resolved NMR spectrum for this compound was recorded at $-20\text{ }^\circ\text{C}$ (Figures S20–S22), consistent with the presence of a single C_1 -symmetric species. For other compounds in this series, this reorganization process appeared to be more facile and the corresponding ^1H NMR spectra all displayed sharp resonances at room temperature (see the SI).

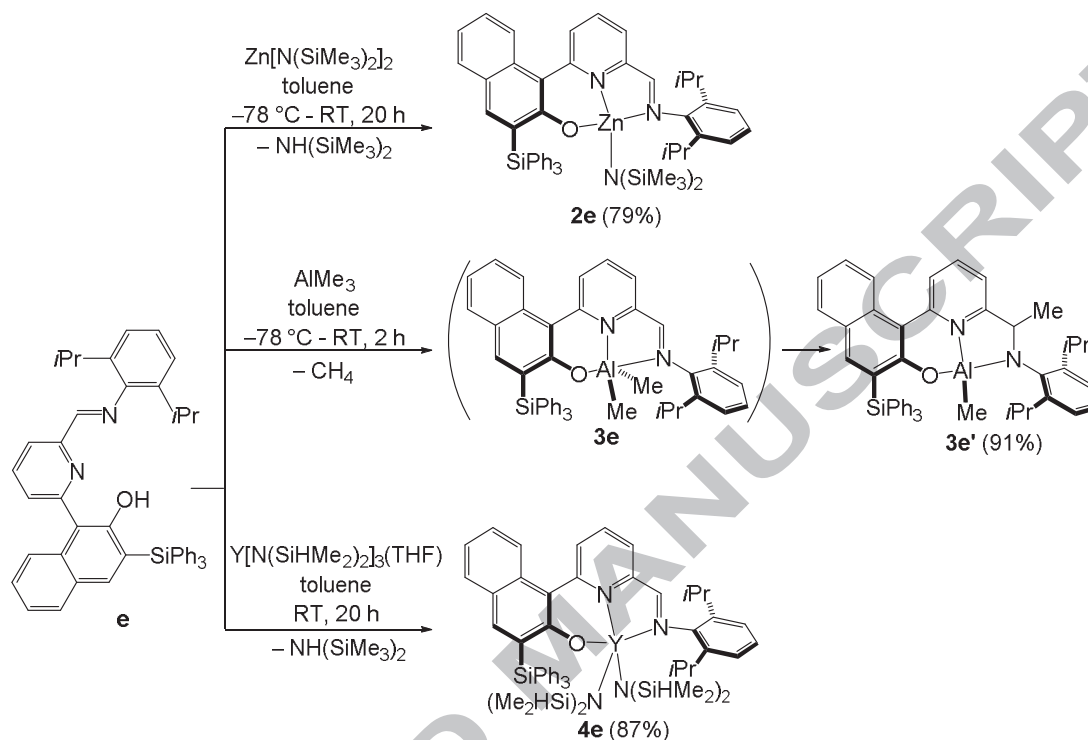
We also investigated the coordination of an {ONO} ligand on group 3 metals through aminolysis of $\text{Ln}[\text{N}(\text{SiHMe}_2)_2]_3\text{THF}$ ($\text{Ln} = \text{Y, La}$) with an equimolar amount of **a**. The reactions were monitored by ^1H NMR spectroscopy in toluene- d_8 at $25\text{ }^\circ\text{C}$. Under these conditions, complete consumption of the proligand, accompanied with concomitant release of 1 equiv of $\text{HN}(\text{SiHMe}_2)_2$, was observed within 18 h for both yttrium and lanthanum. Unfortunately, the ^1H NMR spectra of both products appeared to remain very broad over the large temperature range -50 to $+80\text{ }^\circ\text{C}$, and these NMR data were not conclusive as to the nature of the product(s) formed. Also, all attempts to crystallize these materials failed. Due to these difficulties, the coordination chemistry of other {ONO} ligands with group 3 metals was not further investigated.



Scheme 6. Synthesis of {ONO}⁻ complexes of Zn (**1a–d**, **2d** and **2c**) and Al (**3c**).

2. Ligands of ONN-type. Analogous reactivity studies were performed for the {ONN}-type proligand **e** (Scheme 7). Reaction of **e** with 1 equiv of Zn[N(SiMe₃)₂]₂ gave the desired complex **2e** with high yield. On the other hand, using a similar protocol as that employed for the synthesis of **3c**, the reaction of **e** with 1 equiv of AlMe₃ afforded after a standard workup, instead of the desired **3e**, the monomethyl-aluminum complex **3e'** containing a new dianionic {ONN}²⁻ ligand. This result is in line with previous observations made on the coordination of imino-based ligands on AlMe₃, which typically resulted in nucleophilic addition of a methyl group on the C=N bond.⁹

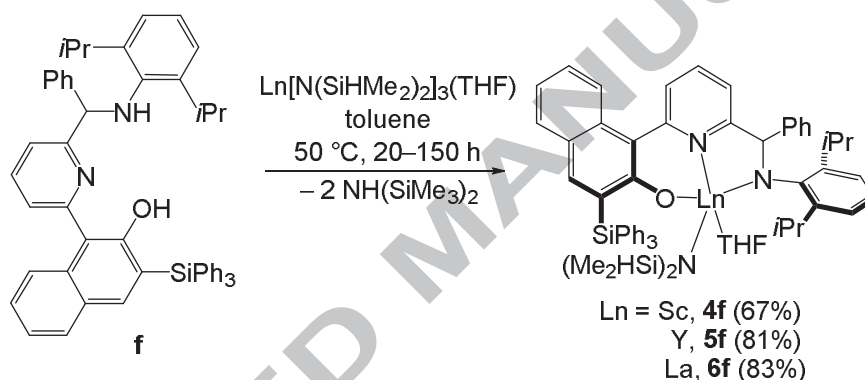
Reaction of **e** with 1 equiv of $Y[N(\text{SiHMe}_2)_2]_3\text{THF}$ successfully yielded the corresponding THF-free diamido compound **4e** (Scheme 7).



Scheme 7. Synthesis of $\{\text{ONN}\}^-$ and $\{\text{ONN}\}^{2-}$ complexes of Zn (**2e**), Al (**3e'**) and Y (**4e**).

Complexes **2e**, **3e'** and **4e** were characterized by ^1H , $^{13}\text{C}\{^1\text{H}\}$ and ^{29}Si (for **4e**) NMR spectroscopy in solution, and elemental analysis and X-ray diffraction study (for **2e**) in the solid state. The fluxional dynamic behavior observed for **2e** and **4e** in benzene solution (Fig. S32, S38 and S40) may arise from hindered rotation associated to the bulky diisopropylphenyl and amido groups. All three complexes featured asymmetric structures in solution, as revealed by ^1H and $^{13}\text{C}\{^1\text{H}\}$ NMR spectroscopy. For instance, the *i*Pr groups of the diisopropylphenyl groups gave rise to two sets of signals in the corresponding NMR spectra. In **4e**, the two $\text{N}(\text{SiHMe}_2)_2$ groups were also found non-equivalent and appeared as two sets of signals in the corresponding ^1H , ^{13}C and ^{29}Si NMR spectra (Figures S38, S39 and S42, respectively); those signals do not coalesce, even upon heating at 60 °C.

The amine elimination reactions between **f** and 1 equiv of $\text{Ln}[\text{N}(\text{SiHMe}_2)_2]_3\text{THF}$ ($\text{Ln} = \text{Sc}, \text{Y}$ and La) were investigated (Scheme 8). The reactions took place at 50 °C overnight with complete consumption of the proligand and concomitant release of 2 equiv of $\text{HN}(\text{SiHMe}_2)_2$ to afford **5f** (Y) and **6f** (La). For the Sc analogue **4f**, an extended reaction time (one week) was required for completion of the reaction. This reactivity trend is in agreement with the larger ionic character of Y and La (Y^{+3} (CN = 6): 0.90 Å, La^{+3} (CN = 6): 1.03 Å) as compared to that of Sc (Sc^{+3} (CN = 6): 0.75 Å).¹⁰ After a standard workup, the monoamido complexes **4–5f** of the dianionic {ONN}-type ligand were isolated in good yields (67–83%).



Scheme 8. Synthesis of {ONN}²⁻ complexes of Sc (**4f**), Y (**5f**) and La (**6f**).

These compounds are readily soluble in aromatic hydrocarbons (benzene, toluene) and in THF. The structures of these complexes were established on the basis of ¹H, ¹³C{¹H}, ²⁹Si{¹H} and ²⁹Si NMR spectroscopy and elemental analysis. By analogy with group 3 metal complexes of dianionic bis(naphthoxy)pyridine ligands,^{5b} the mono-THF adducts **4f–6f** are most probably mononuclear and five-coordinate in benzene or toluene solutions. The chemical shifts of the SiH moiety (δ 4.70–4.84 ppm at room temperature in C₆D₆) for **4f**, **5f** and **6f** and the ¹J_{Si-H} coupling constants (180, 165 and 163 Hz, respectively) were found in the regular range of values, arguing against strong β-Si–H···Ln agostic interactions with the metal centers in solution.¹¹ The structures of all complexes are asymmetric in solution over a broad

temperature range, as judged from the ^1H NMR data obtained for **5f** (Figure S51). Also, no interconversion between asymmetric species having different geometries was evidenced for the latter species by variable-temperature ^1H NMR spectroscopy.¹²

Solid-State Structures of Zinc and Aluminum Complexes. Single crystals of zinc and aluminum complexes suitable for X-ray diffraction analysis were obtained from the following mixtures: C_6H_6 /heptane (**1d**:1.5 C_6H_6), THF/hexane (**1c** and **3c**: $\text{C}_4\text{H}_8\text{O}$) and toluene/hexane (**1a**:0.5 C_7H_8 , **2c** and **2e**). The crystallographic data of these complexes are summarized in Table S3 and important bond distances and angles are given in the corresponding Figures 1–6.

In the solid state, all the complexes feature a monomeric structure with the metal center in a distorted tetrahedral geometry. The common feature observed in these molecular structures lies in the non-coplanarity of the naphthoxy and pyridine planes. The twist angles between these two fragments range from 42.04 to 55.8°, which falls within the range of values (38.7–64.4°) observed for related bis(naphthoxy)pyridine complexes of group 3 and 4 metals.^{3,5}

In zinc complexes **1a**, **1d**, **2c** and **2e**, the metal center lies in a (distorted) tetrahedral environment, coordinated by the tridentate ligands and the ethyl or bis(trimethylsilyl)amido group. In **1c**, the ligand is only κ^2 -coordinated by its O(naphthoxy) and N(pyridine) and the metal center is also four-coordinated by an additional THF molecule (instead of the ligand methoxy, in contrast to **1d**). The Zn–O(naphthoxy) (1.912(4)–1.979(3) Å), Zn–N(pyridine) (2.037(3)–2.133(2) Å), Zn–C(ethyl) (1.956(3)–1.977(3) Å) and Zn–N(amido) (1.9015(16)–1.902(3) Å) bond lengths are in the range of, or are close to those observed in related compounds (2.021(2)–2.029(2),¹³ 1.962(2)–2.054(4),^{7,8,14} 1.958(3)–1.981(2)^{7,14,15} and 1.869(2)–1.920(4) Å,⁸ respectively). Noteworthy, the Zn–N(imino) bond distance in **2e** (2.162(3) Å) is *ca.* 0.1 Å longer than that reported for related compounds (1.872(1)–1.977(4)

Å). This elongation can probably be a result of a significant steric hindrance in **2e**.

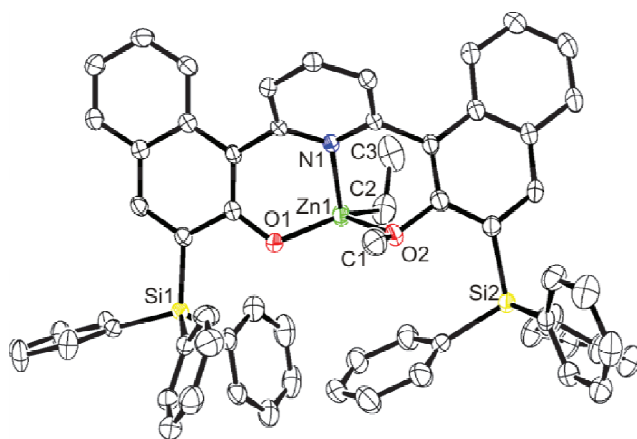


Figure 1. Solid-state molecular structure of **1a**·0.5C₇H₈ (thermal ellipsoids drawn at 50% probability; all solvent molecules and hydrogen atoms are omitted for clarity). Selected bond distances (Å) and angles (deg): Zn(1)–O(1), 1.912(4); Zn(1)–O(2), 2.238(4); Zn(1)–N(1), 2.103(2); Zn(1)–C(2), 1.956(3); Zn(1)–C(2)–C(3), 112.0(2); O(1)–Zn(1)–O(2), 97.2(2); Zn(1)–O(2)–C(1), 125.3(2); O(1)–Zn(1)–N(1), 90.3(7); O(2)–Zn(1)–N(1), 79.5(7); C(2)–Zn(1)–N(1), 116.55(11).

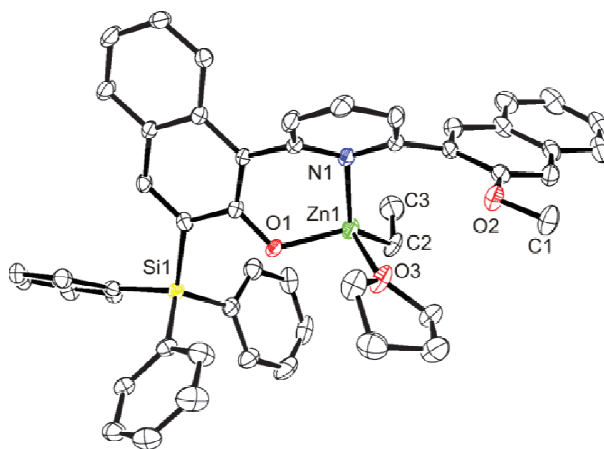


Figure 2. Solid-state molecular structure of **1c** (thermal ellipsoids drawn at 50% probability; all hydrogen atoms are omitted for clarity). Selected bond distances (Å) and angles (deg): Zn(1)–O(1), 1.9386(18); Zn(1)–N(1), 2.133(2); Zn(1)–C(2), 1.977(3); Zn(1)–O(3), 2.138(2); Zn(1)–C(2)–C(3), 119.6(2); O(1)–Zn(1)–O(3), 91.08(8); O(3)–Zn(1)–N(1), 89.60(8); O(1)–Zn(1)–N(1), 91.23(8); C(2)–Zn(1)–N(1), 133.03(11).

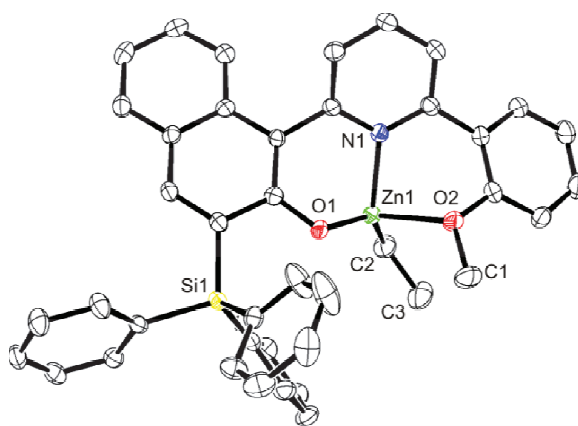


Figure 3. Solid-state molecular structure of **1d**·1.5C₆H₆ (thermal ellipsoids drawn at 50% probability; all solvent molecules and hydrogen atoms are omitted for clarity). Selected bond distances (Å) and angles (deg): Zn(1)–O(1), 1.9390(18); Zn(1)–O(2), 2.265(2); Zn(1)–N(1), 2.065(2); Zn(1)–C(2), 1.960(3); Zn(1)–C(2)–C(3), 116.4(2); O(1)–Zn(1)–O(2), 95.52(8); Zn(1)–O(2)–C(1), 116.23(18); O(1)–Zn(1)–N(1), 88.65(8); O(2)–Zn(1)–N(1), 79.05(8); C(2)–Zn(1)–N(1), 130.94(11).

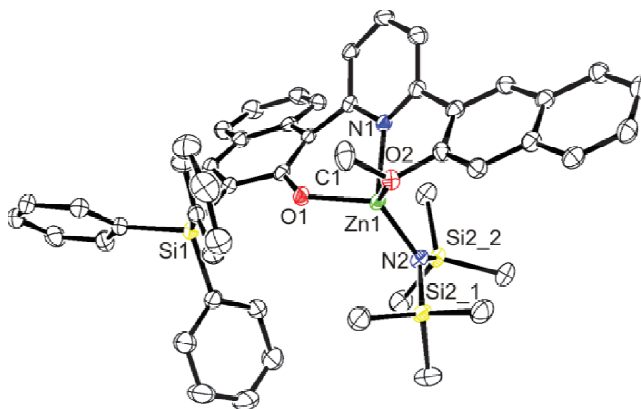


Figure 4. Solid-state molecular structure of **2c** (thermal ellipsoids drawn at 50% probability; all hydrogen atoms are omitted for clarity). Selected bond distances (Å) and angles (deg): Zn(1)–O(1), 1.9363(13); Zn(1)–O(2), 2.1454(13); Zn(1)–N(1), 2.0422(16); Zn(1)–N(2), 1.9015(16); N(1)–Zn(1)–N(2), 131.71(7); O(1)–Zn(1)–O(2), 97.65(5); Zn(1)–O(2)–C(1), 118.08(12); O(1)–Zn(1)–N(1), 90.57(6); O(2)–Zn(1)–N(1), 84.98(6); O(1)–Zn(1)–N(2), 127.68(7), O(2)–Zn(1)–N(2), 112.96(6).

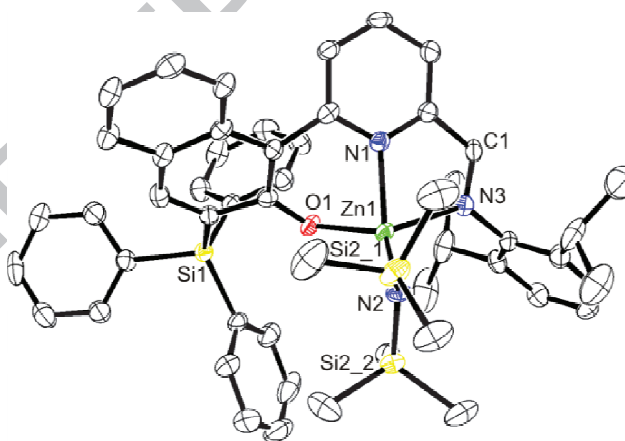


Figure 5. Solid-state molecular structure of **2e** (thermal ellipsoids drawn at 50% probability; all hydrogen atoms are omitted for clarity). Selected bond distances (Å) and angles (deg): Zn(1)–O(1), 1.979(3); Zn(1)–N(1), 2.037(3); Zn(1)–N(2), 1.902(3); Zn(1)–N(3), 2.162(3); N(3)–C(1), 1.276(5); N(1)–Zn(1)–N(2), 130.35(13); O(1)–Zn(1)–N(3), 119.03(11); Zn(1)–

N(3)–C(1), 111.2(3); O(1)–Zn(1)–N(1), 84.80(12); N(1)–Zn(1)–N(3), 78.22(13); O(1)–Zn(1)–N(2), 122.61(13), N(2)–Zn(1)–N(3), 112.51(13).

The overall geometry and metal coordination environment in **3c** are the same as those observed before in four-coordinated dimethyl-aluminum complexes of both bi- and tridentate *o*-Ph₃Si-substituted phenoxy-imino ligands.¹⁶ The Al–O(naphthoxy) (1.781(2) Å), Al–N(pyridine) (2.023(2) Å), and Al–C(methyl) (1.943(3)–1.968(4) Å) bond distances are in the normal range found for the abovementioned complexes (1.772(2)–1.861(3), 2.027(3) and 1.951(2)–1.979(3) Å).¹⁶

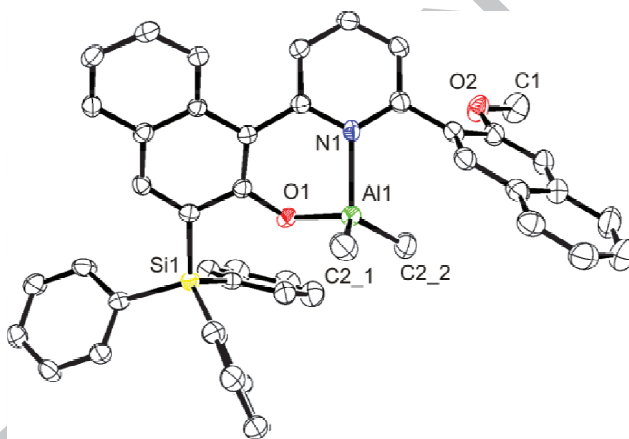


Figure 6. Solid-state molecular structure of **3c**·C₄H₈O (thermal ellipsoids drawn at 50% probability; all solvent molecules and hydrogen atoms are omitted for clarity). Selected bond distances (Å) and angles (deg): Al(1)–O(1), 1.781(2); Al(1)–N(1), 2.023(2); Al(1)–C(2_1), 1.968(4); Al(1)–C(2_2), 1.943(3); O(1)–Al(1)–N(1), 92.13(9); O(1)–Al(1)–C(2_1), 111.78(12); O(1)–Al(1)–C(2_2), 106.12(13), N(1)–Al(1)–C(2_1), 110.30(12); N(1)–Al(1)–C(2_2), 112.21(12).

Recrystallization of **3e'** from a solution in a toluene/hexanes mixture unexpectedly resulted in isolation of crystals of product **3e''**, arising from adventitious hydrolysis of the parent monomethyl complex. The molecular structure of **3e''** is depicted in Figure 7. In the oxo-bridged structure of this molecule, each of the two tetrahedral aluminum centers is κ^3 -coordinated by a tridentate ligand. The Al–O and Al–N bond lengths in **3e''** are comparable to those observed in **3c** and other related complexes of *o*-Ph₃Si-substituted phenoxy-imino ligands.¹⁶

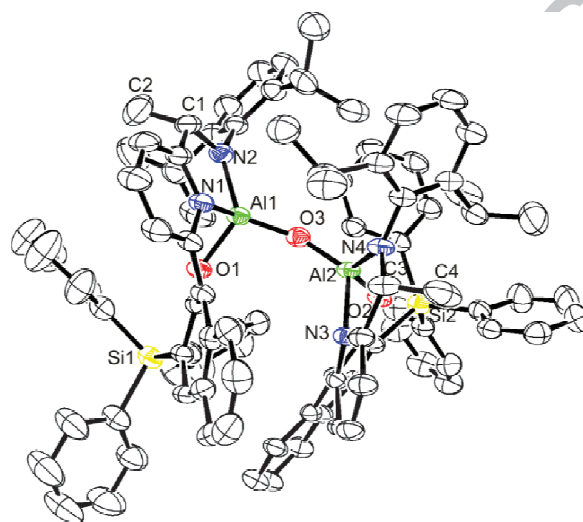


Figure 7. Solid-state molecular structure of **3e''** (thermal ellipsoids drawn at 50% probability; all hydrogen atoms are omitted for clarity). Selected bond distances (Å) and angles (deg): Al(1)–O(1), 1.7794(15); Al(1)–N(1), 1.9318(17); Al(1)–N(2), 1.817(2); N(2)–C(1), 1.473(3); Al(1)–O(3), 1.690(2); N(1)–Al(1)–N(2), 86.52(8); O(1)–Al(1)–N(1), 89.15(7); Al(1)–N(2)–C(1), 115.64(14); N(2)–C(1)–C(2), 112.6(2); O(1)–Al(1)–N(2), 124.66(8), Al(1)–O(3)–Al(2), 154.80(9).

Studies on Ring-Opening Polymerization of *rac*-Lactide (*rac*-LA) and *rac*-Butyrolactone (*rac*-BBL). The new zinc, aluminum and group 3 metals complexes have

potentially active nucleophilic groups (i.e., alkyl and amido) and their performances as initiators of the ROP of *racemic* lactide and β -butyrolactone were assessed. Representative results are summarized in Tables 1 and 2.

(insert Table 1 here)

Zinc-based Initiators. Not surprisingly in light of the poor nucleophilicity of the ethyl group, zinc ethyl complexes **1a**, **1c** and **1d** proved to be quite poor initiators in the ROP of *rac*-LA. The polymerization did not take place at room temperature and substantial heating (60–100 °C) was required to achieve high conversions. Complex **1a** containing the Ph₃Si-disubstituted bis(naphthoxy) ligand was not active even under these conditions (Table 1, entries 1 and 2). When combined with isopropanol (5 equiv), **1a** appeared to be active at 100 °C, slowly converting 100 and 1,000 equiv of lactide (entries 3 and 4, respectively). The atactic PLAs formed under those conditions had unimodal, although broadened molecular distributions with the experimental number-average molecular weights being close to the calculated ones (based on the converted monomer-to-alcohol ratio).

Complexes with the less bulky ligands **1c** and **1d** exhibited higher activity than **1a** and enabled the conversion of 100 equiv of *rac*-lactide within a few minutes at 80 °C in toluene or at 60°C in THF solution, even without addition of isopropanol (entries 6, 7 and 5, respectively). The resulting slightly heterotactic-enriched PLAs ($P_r = 0.65$ – 0.75) have relatively broad molecular distributions ($\mathcal{D}_M = 1.5$ – 2.1).

As expected, the more nucleophilic amide-zinc complexes **2c**, **2d** and **2e** proved to be active at room temperature, enabling the conversion of 100–2,000 equiv of *rac*-LA within relatively short periods of time (entries 8–12, 15–17). The PLAs obtained with **2c** and **2d** under these conditions had also unimodal, yet rather broad molecular weight distributions ($\mathcal{D}_M = 1.3$ – 2.0), which argues for their unoptimal initiation efficiency and/or propensity to promote side-reactions such as transesterification. Remarkably, **2e** even without *i*PrOH (entries 16 and 17) afforded PLAs with rather narrow polydispersities ($\mathcal{D}_M = 1.11$) and good agreement

between the experimental and calculated molecular weights. The presence of isopropanol turned out to be detrimental for the activities of these systems. For instance, the combinations of **2c** or **2e** with *i*PrOH (one equiv) were completely inactive at room temperature (entries 13, 18 and 19). Actually, an NMR monitoring of the reaction of **2c** with one equiv of isopropanol in toluene-*d*₈ at room temperature indicated decomposition of the complex with release of *protio c*. Homo-decoupled ¹H NMR spectroscopy showed that the PLAs obtained with systems **2c**, **2d** and **2e** all had a slightly heterotactic-enriched microstructures ($P_r = 0.65\text{--}0.76$).

The performance of **2c** and **2e**, the most active complexes towards *rac*-LA, were next assessed in the ROP of *rac*-BBL. Polymerization occurred only upon heating at 60–80 °C and complete conversions were reached after longer time periods (Table 2, entries 2 and 3). Despite the absence of co-initiator / chain-transfer agent (*i*PrOH), the initiation with these systems appeared remarkably efficient and PHBs featuring narrow molecular weight distributions were isolated ($\mathcal{D}_M = 1.07\text{--}1.23$). Yet, the experimental number average molecular weights were not systematically close to the calculated ones. Also, polymerizations with **2c** and **2e** were found to be essentially nonstereoselective.

(insert Table 2 here)

Aluminum-based Initiators. ROP of *rac*-LA with dimethyl-aluminum **3c** and monomethyl-aluminum **3e'** proceeded at 100 °C in toluene (Table 1, entries 20–23). In general, a good control over the polymerization was achieved with both systems in the presence of isopropanol, as evidenced by the relatively narrow molecular weight distribution of the resulting polymers ($\mathcal{D}_M = 1.17\text{--}1.37$) and the good agreement between observed and theoretical molecular weights calculated on the assumption of the growth on one macromolecular chain per metal center. The homo-decoupled ¹H NMR experiments conducted on the PLAs samples produced with these aluminum compounds indicated that all

of them are atactic. On the other hand, complexes **3c** and **3e'** were found completely inactive towards *rac*-BBL (Table 2, entries 7–9), which is not unsurprising for aluminum complexes.¹

Group 3 Metal-based Initiators. The group 3 diamido **4e** and monoamido **5f** and **6f** were found very active toward the ROP of *rac*-LA at room temperature (Table 1, entries 24–28, 30–35); nearly quantitative conversions of the monomer were achieved within a few minutes (for **4e**, TOF up to 1840 mol(LA)·mol(Y)⁻¹·h⁻¹ at 25 °C). Without the addition of isopropanol, yttrium compound **4e** gave PLAs with broad molecular weight distributions ($\mathcal{D}_M = 2.1$, entries 24–26) and number-average molecular weight values generally twice larger with respect to those calculated from the monomer-to-yttrium ratio. The reactions proceeded even faster in the presence of isopropanol (compare entries 24/27 and 26/28) and all the PLAs formed under those conditions had unimodal narrow molecular distributions ($\mathcal{D}_M = 1.21$ – 1.35) and experimental number-average molecular weights (M_n) quite close to the calculated values (entries 27 and 28), indicating a more controlled behavior.

Within the **f** series, the activity of complexes clearly follows the order of ionic radii of metals La(**6f**) > Y(**5f**) > Sc(**4f**). Thus, for scandium complex **4f**, a substantial heating was required to achieve a good conversion (entry 29). Such trend was already observed for a similar series of group 3 metal amino-alkoxy-bis(phenolate) complexes and was explained on account of a more sterically hindered metal center.¹⁷ These lanthanide systems provided relatively broad molecular weight distributions ($\mathcal{D}_M = 1.4$ – 2.0), which do not improve much if isopropanol is used as chain-transfer agent (compare entries 30/33 and 34/35). Homo-decoupled ¹H NMR spectroscopy showed that the PLAs formed with these systems have heterotactic-enriched microstructures with the probability of racemic linkage ranging from 0.78–0.80 for **4e** to 0.57–0.69 for **4–6f**.

In line with previous reports,^{5b,17} the activities of complexes **4e** and **4–6f** in the ROP of *rac*-BBL were found inferior to those of *rac*-LA (Table 2, entries 10–14). For instance, polymerization reactions with **5f** and **6f** required longer periods of time, while with **4f** they

did not take place at all even at 60 °C. For the most active **4e**, the TOF was up to 900 mol(BBL)·mol(Y)⁻¹·h⁻¹ at 25 °C. The resulting PHBs had molecular weight distributions that were unimodal, although somewhat large ($\bar{M}_w = 1.5\text{--}1.9$). None of these complexes proved to be stereoselective, giving mostly atactic PHB polymers ($P_r = 0.42\text{--}0.66$).

Conclusions

Several new series of bulky Ph₃Si-substituted tridentate naphthol-pyridine proligands have been conveniently prepared and straightforwardly installed onto Zn, Al and group 3 metals (Sc, Y and La) as alkyl and amido complexes. These monomeric and monometallic complexes all adopt C₁-symmetry both in the solid state and in solution (benzene, toluene or THF).

Studies in the ROP of *rac*-LA and *rac*-BBL indicated that some of these systems exhibit significant activity, good molecular weight control and narrow molecular weight distributions. On the other hand, modest degrees of stereocontrol were achieved with these systems. The performances of the complexes obtained in this study compare well with that of their corresponding imino-phenoxide and related analogues.^{5b,15,16,18}

Experimental Section

General Considerations. All manipulations were performed under a purified argon atmosphere using standard Schlenk techniques or in a glovebox (< 1 ppm O₂, < 5 ppm H₂O). Solvents were distilled from Na/benzophenone (THF, Et₂O) or Na/K alloy (toluene, hexane and pentane) under argon, degassed thoroughly and stored under argon prior to use. Deuterated solvents were stored over Na/K alloy (benzene-*d*₆, toluene-*d*₈, THF-*d*₈; >99.5% D, Eurisotop) and vacuum-transferred just before use. CDCl₃ was dried over a mixture of 3 and 4 Å molecular sieves. Precursors Ln[N(SiHMe₂)₂]₃(THF) (Ln = Sc, Y, La)¹⁹ and Zn[N(SiMe₃)₂]₂²⁰ were prepared as described in the literature. Other starting materials were

purchased from Acros, Strem, Alfa and Aldrich and used as received. *Racemic* lactide (*rac*-LA) and *racemic* β -butyrolactone (*rac*-BBL) were received from Aldrich and TCI, respectively. Purification of *rac*-LA required a three-step procedure involving first a recrystallization from a hot, concentrated *i*PrOH solution (80 °C), followed by two subsequent recrystallizations in hot toluene (100 °C). *Rac*-BBL was freshly distilled from CaH₂ under nitrogen and degassed thoroughly by freeze-thaw-vacuum cycles prior to use. After purification, *rac*-LA and *rac*-BBL were stored at -30 °C in the glove-box.

Instrumentation and Measurements. NMR spectra of complexes were recorded on Bruker Avance DRX 400 and AM-500 spectrometers in Teflon-valved NMR tubes at 25 °C unless otherwise indicated. ¹H and ¹³C NMR chemical shifts are reported in ppm vs. SiMe₄ and were determined by reference to the residual solvent peaks. Assignment of resonances for organometallic complexes was made from 2D ¹H-¹³C HMQC and HMBC NMR experiments. ²⁹Si chemical shifts were determined with respect to the external reference (Me₄Si).

Elemental analyses (C, H, N) were performed on recrystallized samples that were thoroughly dried under vacuum, using a Flash EA1112 CHNS Thermo Electron apparatus and are the average of two independent determinations.

Size exclusion chromatography (SEC) analyses of PLAs and PHBs were performed in THF (1.0 mL.min⁻¹) at 20 °C using a Polymer Laboratories PL-GPC 50 plus apparatus equipped with two ResiPore 300 × 7.5 mm columns, and RI and Dual angle LS (PL-LS 45/90) detectors. The number-average molecular masses (*M_n*) and polydispersity index (*M_w/M_n*) of the polymers were calculated with reference to a universal calibration vs. polystyrene standards. Reported experimental SEC molar mass values (*M_{n,SEC}*) for PLA samples were corrected by a factor of 0.58 as previously established;²¹ those of PHBs are uncorrected. Unless otherwise stated, the SEC traces of the polymers all exhibited a unimodal, and usually symmetrical, peak.

(3-(Methoxymethoxy)-4-(4,4,5,5-tetramethyl-1,3,2-dioxaborolan-2-

yl)naphthalen-2-yl)triphenylsilane. To a solution of [3-(methoxymethoxy)-2-naphthyl](triphenylsilane)³ (5.00 g, 11.19 mmol) in THF (100 mL) was added TMEDA (1.67 mL, 11.21 mmol) followed by addition of *sec*-BuLi (9.12 mL of a 1.3 M solution in hexane/cyclohexane, 11.86 mmol) at -78 °C. The reaction mixture was stirred at room temperature overnight. Then, 2-isopropoxy-4,4,5,5-tetramethyl-1,3,2-dioxaborolane (3.65 mL, 17.90 mmol) was added via syringe at -78 °C. After 30 min at -78 °C, the flask was removed from the cooling bath and allowed to warm to room temperature while stirring; the reaction mixture was stirred at 70 °C overnight. The reaction was quenched with saturated aqueous ammonium chloride and extracted with CH_2Cl_2 (3×50 mL). The combined organic layers were dried over magnesium sulfate and evaporated to yield a yellowish solid. The product was purified by passing through a short silica column using CH_2Cl_2 as eluent, to afford the product as an off-white solid (5.45 g, 85%). ¹H NMR (500 MHz, CDCl_3 , 298 K): δ 8.00 (d, $^3J_{H-H} = 8.4$, 1H, aryl-CH), 7.76 (s, 1H, aryl-CH), 7.61 (d, $^3J_{H-H} = 7.6$, 6H, aryl-CH), 7.47–7.44 (m, 1H, aryl-CH), 7.41–7.38 (m, 4H, aryl-CH), 7.36–7.33 (m, 6H, aryl-CH), 7.31–7.28 (m, 1H, aryl-CH), 4.67 (s, 2H, CH_2OCH_3), 2.89 (s, 3H, CH_2OCH_3), 1.48 (s, 12H, $\text{BOC}(\text{CH}_3)_2$). ¹³C NMR (125 MHz, CDCl_3 , 298 K): δ 162.2 (aryl-Cq), 142.3 (aryl-CH), 139.0 (aryl-Cq), 136.4 (aryl-CH), 136.3 (aryl-CH), 135.2 (aryl-Cq), 129.4 (aryl-Cq), 129.2 (aryl-CH), 128.8 (aryl-CH), 128.1 (aryl-CH), 127.6 (aryl-CH), 127.0 (aryl-CH), 126.9 (aryl-Cq), 126.6 (aryl-CH), 123.8 (aryl-CH), 96.0 (CH_2OCH_3), 84.3 ($\text{BOC}(\text{CH}_3)_2$), 55.4 (CH_2OCH_3), 25.9 ($\text{BOC}(\text{CH}_3)_2$). Anal. Calcd for $\text{C}_{36}\text{H}_{37}\text{BO}_4\text{Si}$: C, 75.52; H, 6.51. Found: C, 75.48; H, 6.54.

2-Bromo-6-(2-(methoxymethoxy)-3-(triphenylsilyl)naphthalen-1-yl)pyridine. An oven-dried 250 mL Schlenk flask, equipped with a stirring bar and a Teflon valve, was charged with 2,6-dimethylpyridine (2.47 g, 10.47 mmol), (3-(methoxymethoxy)-4-(4,4,5,5-tetramethyl-1,3,2-dioxaborolan-2-yl)naphthalen-2-yl)triphenylsilane (5.45 g, 9.52 mmol),

Pd(PPh₃)₄ (0.55 g, 0.47 mmol) and K₃PO₄ (4.05 g, 19.11 mmol) under argon. Then, dry toluene (100 mL) was added via syringe. The reaction mixture was stirred at room temperature for 30 min, during this time the bright yellow color faded to pale yellow (with insoluble white K₃PO₄). The flask was placed in an oil bath at 115 °C with stirring for 3 days. Then, the reaction mixture was cooled to room temperature and the suspension was filtered through celite with the aid of Et₂O. Volatiles were removed under vacuum and the resulting residue was purified by recrystallization using an Et₂O/CH₂Cl₂ mixture (1:1) to give a solid (3.00 g, 52%). ¹H NMR (500 MHz, CDCl₃, 298 K): δ 7.88 (s, 1H, aryl-CH), 7.69–7.67 (m, 2H, aryl-CH), 7.64 (d, ³J_{H-H} = 7.4, 7H, aryl-CH), 7.53–7.47 (m, 3H, aryl-CH), 7.43–7.42 (m, 3H, aryl-CH), 7.39–7.37 (m, 1H, aryl-CH), 3.91 (s, 2H, CH₂OCH₃), 2.62 (s, 3H, CH₂OCH₃). ¹³C NMR (125 MHz, CDCl₃, 298 K): δ 157.9 (aryl-Cq), 157.2 (aryl-Cq), 141.6 (aryl-CH), 141.4 (aryl-Cq), 138.6 (aryl-CH), 136.5 (aryl-CH), 134.8 (aryl-Cq), 134.6 (aryl-Cq), 130.2 (aryl-Cq), 129.5 (aryl-CH), 128.9 (aryl-Cq), 128.5 (aryl-CH), 127.8 (aryl-CH), 127.7 (aryl-CH), 126.7 (aryl-Cq), 126.6 (aryl-CH), 125.9 (aryl-CH), 124.9 (aryl-CH), 124.8 (aryl-CH), 99.4 (CH₂OCH₃), 56.0 (CH₂OCH₃). Anal. Calcd for C₃₅H₂₈BrNO₂Si: C, 69.76; H, 4.68; N, 2.32. Found: C, 69.72; H, 4.56; N, 2.30.

6-(2-(Methoxymethoxy)-3-(triphenylsilyl)naphthalen-1-yl)picolinaldehyde. (3-(Methoxymethoxy)-4-(4,4,5,5-tetramethyl-1,3,2-dioxaborolan-2-yl)naphthalen-2-yl)triphenylsilane (5.00 g, 8.7 mmol) and Na₂CO₃ (1.91 g, 18.1 mmol) were dissolved in a degassed H₂O/MeOH mixture (4:1, 60 mL). The resulting solution was added via cannula to a solution of 6-bromopicolinaldehyde (1.35 g, 7.2 mmol) and Pd(PPh₃)₄ (416 mg, 0.36 mmol) in degassed toluene (50 mL). The biphasic mixture was heated to 90 °C for 48 h under vigorous stirring. After cooling to room temperature, the organic phase was separated and washed with Et₂O (3 × 25 mL). The combined organic extracts were washed with H₂O (3 × 25 mL) and brine (1 × 20 mL), and dried over Na₂SO₄. Volatiles were removed under vacuum, and the resulting brown oil was chromatographed on silica using CH₂Cl₂ as eluent.

The early fractions containing (3-(methoxymethoxy)-4-(4,4,5,5-tetramethyl-1,3,2-dioxaborolan-2-yl)naphthalen-2-yl)triphenylsilane and 6-bromopicolinaldehyde were separated. The remaining fractions were combined and volatiles were removed under vacuum to provide 6-(2-(methoxymethoxy)-3-(triphenylsilyl)naphthalen-1-yl)picolinaldehyde as a yellow solid (2.50 g, 63%). ^1H NMR (500 MHz, CDCl_3 , 298 K): δ 10.19 (s, 1H, CHO), 8.04–8.03 (m, 1H, aryl-CH), 7.96 (s, 1H, aryl-CH), 7.79–7.75 (m, 2H, aryl-CH), 7.70–7.68 (m, 6H, aryl-CH), 7.49–7.40 (m, 13H, aryl-CH), 3.89 (br s, 2H, CH_2OCH_3), 2.55 (s, 3H, CH_2OCH_3). ^{13}C NMR (125 MHz, CDCl_3 , 298 K): δ 193.7 (CHO), 157.7 (aryl-Cq), 157.5 (aryl-Cq), 152.6 (aryl-Cq), 141.7 (aryl-CH), 137.3 (aryl-CH), 136.5 (aryl-CH), 134.7 (aryl-Cq), 134.6 (aryl-Cq), 131.6 (aryl-CH), 130.4 (aryl-Cq), 129.6 (aryl-CH), 129.1 (aryl-Cq), 128.7 (aryl-CH), 127.9 (aryl-CH), 127.8 (aryl-CH), 127.1 (aryl-Cq), 125.0 (aryl-CH), 124.6 (aryl-CH), 120.0 (aryl-CH), 99.5 (CH_2OCH_3), 55.9(CH_2OCH_3). Anal. Calcd for $\text{C}_{36}\text{H}_{29}\text{NO}_3\text{Si}$: C, 78.37; H, 5.30; N, 2.54. Found: C, 78.42; H, 5.35; N, 2.60.

6-(2-Hydroxy-3-(triphenylsilyl)naphthalen-1-yl)picolinaldehyde. 6-(2-(Methoxymethoxy)-3-(triphenylsilyl)naphthalen-1-yl)picolinaldehyde (2.50 g, 4.53 mmol) was dissolved in a mixture of concentrated HCl (20 mL), CHCl_3 (30 mL), and EtOH (40 mL), and the solution was refluxed for 4 h. The reaction mixture was cooled to 0 °C and then carefully diluted with a concentrated solution of NaOH (50 mL). Then, a concentrated solution of NH_4Cl was added to adjust the pH value to 7–8. The product was extracted with CH_2Cl_2 (3 \times 20 mL), and the combined organic extracts were dried over MgSO_4 and evaporated to afford the desired compound as a yellow solid (1.20 g, 52%). ^1H NMR (400 MHz, CDCl_3 , 298 K): δ 12.01 (s, 1H, OH), 10.09 (s, 1H, CHO), 8.28 (d, $^3J_{\text{H-H}} = 8.6$ Hz, 1H, aryl-CH), 8.14 (t, $^3J_{\text{H-H}} = 8.1$, 2H, aryl-CH), 8.00–7.92 (m, 5H, aryl-CH), 7.85 (d, $^3J_{\text{H-H}} = 6.5$, 5H, aryl-CH), 7.76 (d, $^3J_{\text{H-H}} = 7.9$, 1H, aryl-CH), 7.73 (d, $^3J_{\text{H-H}} = 8.1$, 1H, aryl-CH), 7.65 (d, $^3J_{\text{H-H}} = 7.4$, 1H, aryl-CH), 7.55–7.45 (m, 5H, aryl-CH), 7.39–7.32 (m, 2H, aryl-CH).

Proligand a. A Schlenk flask was charged with a 1,1'-(pyridine-2,6-diyl)bis(3-(triphenylsilyl)naphthalen-2-ol)³ (1.00 g, 1.13 mmol) and PhCH₂K (0.148 g, 1.13 mmol), and THF (*ca.* 10 mL) was vacuum transferred in at -78 °C. The reaction mixture was gently warmed to room temperature and stirred for 2 h at 60 °C. To this mixture, MeI (77.8 μ L, 1.25 mmol) was added dropwise at -78 °C. The reaction mixture was stirred for 24 h at 60 °C, cooled to room temperature, diluted with water (50 mL), and extracted with CH₂Cl₂ (3 \times 20 mL). The combined organic extracts were dried over MgSO₄ and evaporated to dryness. The crude material contained *ca.* 50% of the desired product, 1-(6-(2-methoxy-3-(triphenylsilyl)naphthalen-1-yl)pyridin-2-yl)-3-(triphenylsilyl)naphthalen-2-ol, as judged by ¹H NMR spectroscopy. This crude material was purified by column chromatography (silica, heptane/EtOAc (9:1), *R_f* = 0.10) and recrystallized from an heptane/EtOAc (9:1) mixture to give, after drying under vacuum, an analytically pure yellow microcrystalline material (0.50 g, 49%). ¹H NMR (400 MHz, CDCl₃, 298 K): δ 12.87 (br s, 1H, OH), 8.22 (d, ³*J_{H-H}* = 8.6, 1H, aryl-CH), 7.91–7.87 (m, 2H, aryl-CH), 7.78 (s, 1H, aryl-CH), 7.67 (s, 1H, aryl-CH), 7.64–7.60 (m, 2H, aryl-CH), 7.56–7.51 (m, 12H, aryl-CH), 7.44–7.39 (m, 2H, aryl-CH), 7.32–7.16 (m, 22H, aryl-CH), 2.29 (s, 3H, OCH₃). ¹³C NMR (100 MHz, CDCl₃, 298 K): δ 160.5 (aryl-Cq), 160.4 (aryl-Cq), 156.9 (aryl-Cq), 154.1 (aryl-Cq), 142.8 (aryl-CH), 141.1 (aryl-CH), 137.2 (aryl-CH), 136.6 (aryl-CH), 136.4 (aryl-CH), 134.8 (aryl-Cq), 134.7 (aryl-Cq), 134.6 (aryl-Cq), 133.2 (aryl-Cq), 130.2 (aryl-Cq), 129.4 (aryl-CH), 129.3 (aryl-CH), 129.2 (aryl-CH), 129.1 (aryl-Cq), 128.8 (aryl-Cq), 128.7 (aryl-CH), 127.8 (aryl-CH), 127.7 (aryl-CH), 127.6 (aryl-CH), 125.9 (aryl-Cq), 125.2 (aryl-Cq), 124.7 (aryl-CH), 124.6 (aryl-CH), 124.5 (aryl-CH), 124.4 (aryl-CH), 123.6 (aryl-CH), 122.8 (aryl-CH), 113.0 (aryl-Cq), 60.4 (CH₃). Anal. Calcd for C₆₂H₄₇NO₂Si₂: C, 83.28; H, 5.30; N, 1.57. Found: C, 83.35; H, 5.16; N, 1.53.

Proligand b. Using a procedure similar to that described above for **a**, proligand **b** was obtained 1,1'-(pyridine-2,6-diyl)bis(3-(triphenylsilyl)naphthalen-2-ol) (1.00 g, 1.13

mmol), PhCH₂K (0.148 g, 1.13 mmol), Bu₄NI (0.461 g, 1.25 mmol) and BnBr (148.5 μL, 1.25 mmol). The crude material contained *ca.* 50% of desired product, 1-(6-(2-(benzyloxy)-3-(triphenylsilyl)naphthalen-1-yl)pyridin-2-yl)-3-(triphenylsilyl)naphthalen-2-ol, as judged by ¹H NMR spectroscopy. This crude material was purified by column chromatography (silica, heptane/toluene (6:4), R_f = 0.33). Pure compound **b** was recovered as a pale yellow powder (0.50 g, 46%). ¹H NMR (400 MHz, CDCl₃, 298 K): δ 12.94 (s, 1H, OH), 8.15 (d, ³J_{H-H} = 8.5, 1H, aryl-CH), 7.84 (s, 1H, aryl-CH), 7.72 (d, ³J_{H-H} = 8.0, 1H, aryl-CH), 7.68 (s, 1H, aryl-CH), 7.62 (d, ³J_{H-H} = 7.4, 1H, aryl-CH), 7.63–7.52 (m, 16H, aryl-CH), 7.41–7.37 (m, 1H, aryl-CH), 7.32–7.15 (m, 21H, aryl-CH), 6.88 (t, ³J_{H-H} = 7.3, 1H, OCH₂Ph), 6.78 (t, ³J_{H-H} = 7.5, 2H, OCH₂Ph), 6.23 (d, ³J_{H-H} = 7.3, 2H, OCH₂Ph), 3.81 (s, 2H, OCH₂Ph). ¹³C NMR (100 MHz, CDCl₃, 298 K): δ 160.4 (aryl-Cq), 159.4 (aryl-Cq), 156.5 (aryl-Cq), 154.0 (aryl-Cq), 142.8 (aryl-CH), 141.4 (aryl-CH), 137.5 (aryl-Cq), 137.1 (aryl-CH), 136.6 (aryl-CH), 136.5 (aryl-CH), 134.8 (aryl-Cq), 134.7 (aryl-Cq), 134.6 (aryl-Cq), 133.2 (aryl-Cq), 130.3 (aryl-Cq), 129.5 (aryl-CH), 129.4 (aryl-CH), 129.3 (aryl-CH), 129.0 (aryl-Cq), 128.9 (aryl-Cq), 128.7 (aryl-CH), 127.8 (aryl-CH), 127.7 (aryl-CH), 127.6 (aryl-CH), 127.3 (aryl-CH, OCH₂Ph), 127.1 (aryl-Cq, OCH₂Ph), 126.6 (aryl-CH, OCH₂Ph), 126.2 (aryl-CH, OCH₂Ph), 125.2 (aryl-Cq), 125.1 (aryl-CH), 124.7 (aryl-CH), 124.6 (aryl-CH), 124.5 (aryl-CH), 123.7 (aryl-CH), 122.9 (aryl-CH), 113.3 (aryl-Cq), 75.9 (OCH₂Ph). Anal. Calcd for C₆₈H₅₁NO₂Si₂: C, 84.17; H, 5.30; N, 1.44. Found: C, 84.55; H, 5.22; N, 1.47. Yellow crystals of **b** suitable for X-ray diffraction analysis were obtained by prolonged crystallization from CHCl₃ at room temperature.

Proligand c. A solution of 2-bromo-6-(2-(methoxymethoxy)-3-(triphenylsilyl)naphthalen-1-yl)pyridine (1.00 g, 1.66 mmol), (3-methoxynaphthalen-2-yl)boronic acid (0.335 g, 1.66 mmol), Na₂CO₃ (20 mL of a 2 M solution in water), EtOH (20 mL) and toluene (50 mL) was stirred under argon. After 20 min, Pd(PPh₃)₄ (0.095 g, 0.08 mmol) was added and the solution was refluxed at 90 °C for 48 h. The reaction mixture was

allowed to cool down to room temperature, added to water (50 mL), and extracted with CH_2Cl_2 (3×50 mL). The combined organic layers were dried over magnesium sulfate and evaporated to yield a yellow solid. This solid was dissolved in a mixture of concentrated HCl (20 mL), CHCl_3 (30 mL), and EtOH (40 mL), and the solution was refluxed for 4 h. The reaction mixture was cooled to 0 °C and then carefully diluted with a concentrated solution of NaOH (50 mL). Then, a concentrated solution of NH_4Cl was added to adjust the pH value to 7–8. The product was extracted with CH_2Cl_2 (3×20 mL), and the combined organic extracts were dried over MgSO_4 and evaporated to afford desired compound as a yellow solid. This material was recrystallized using a $\text{Et}_2\text{O}/\text{CH}_2\text{Cl}_2$ mixture (9:1) to afford pure **c** (0.70 g, 66%). ^1H NMR (400 MHz, CDCl_3 , 298 K): δ 12.56 (br s, 1H, OH), 8.25 (d, $^3J_{\text{H-H}} = 8.5$, 1H, aryl-CH), 8.06 (s, 1H, aryl-CH), 7.95 (t, $^3J_{\text{H-H}} = 7.8$, 1H, aryl-CH), 7.87 (d, $^3J_{\text{H-H}} = 7.9$, 1H, aryl-CH), 7.83–7.81 (m, 2H, aryl-CH), 7.74 (d, $^3J_{\text{H-H}} = 6.8$, 7H, aryl-CH), 7.69–7.67 (m, 2H, aryl-CH), 7.49–7.46 (m, 2H, aryl-CH), 7.44–7.37 (m, 10H, aryl-CH), 7.29 (t, $^3J_{\text{H-H}} = 7.4$, 1H, aryl-CH), 7.18 (s, 1H, aryl-CH), 3.57 (s, 3H, OCH_3). ^{13}C NMR (100 MHz, CDCl_3 , 298 K): δ 159.6 (aryl-Cq), 155.9 (aryl-Cq), 155.5 (aryl-Cq), 155.2 (aryl-Cq), 142.3 (aryl-CH), 137.5 (aryl-CH), 136.5 (aryl-CH), 135.2 (aryl-CH), 135.1 (aryl-CH), 134.8 (aryl-Cq), 133.2 (aryl-Cq), 130.7 (aryl-CH), 130.6 (aryl-CH), 129.5 (aryl-Cq), 129.4 (aryl-CH), 129.2 (aryl-CH), 128.8 (aryl-Cq), 128.6 (aryl-Cq), 128.1 (aryl-CH), 127.7 (aryl-CH), 127.1 (aryl-CH), 126.4 (aryl-CH), 125.4 (aryl-Cq), 124.3 (aryl-CH), 124.2 (aryl-CH), 123.5 (aryl-CH), 122.8 (aryl-CH), 121.9 (aryl-CH), 114.7 (aryl-Cq), 106.3 (aryl-CH), 55.0 (CH_3). Anal. Calcd for $\text{C}_{44}\text{H}_{33}\text{NO}_2\text{Si}$: C, 83.12; H, 5.23; N, 2.20. Found: C, 83.10; H, 5.19; N, 2.28.

Proligand d. Using a procedure similar to that described above for **c**, compound **d** was obtained from 2-bromo-6-(2-(methoxymethoxy)-3-(triphenylsilyl)naphthalen-1-yl)pyridine (1.00 g, 1.66 mmol), 2-methoxyphenylboronic acid (0.252 g, 1.66 mmol) and $\text{Pd}(\text{PPh}_3)_4$ (0.095 g, 0.08 mmol). The resulting yellow solid was washed with pentane and recrystallized from CH_2Cl_2 to afford **d** (0.91 g, 93%). ^1H NMR (400 MHz, CDCl_3 , 298 K): δ

12.55 (s, 1H, OH), 8.24 (d, $^3J_{H-H} = 8.5$, 1H, aryl-CH), 7.92 (t, $^3J_{H-H} = 7.8$, 1H, aryl-CH), 7.84 (d, $^3J_{H-H} = 8.9$, 2H, aryl-CH), 7.74 (d, $^3J_{H-H} = 7.7$, 6H, aryl-CH), 7.67 (d, $^3J_{H-H} = 8.1$, 1H, aryl-CH), 7.61–7.57 (m, 2H, aryl-CH), 7.48–7.38 (m, 11H, aryl-CH), 7.29 (t, $^3J_{H-H} = 7.4$, 1H, aryl-CH), 7.06 (t, $^3J_{H-H} = 7.5$, 1H, aryl-CH), 6.95 (d, $^3J_{H-H} = 8.3$, 1H, aryl-CH), 3.49 (s, 3H, OCH₃). ¹³C NMR (125 MHz, CDCl₃, 298 K): δ 159.6 (aryl-Cq), 157.0 (aryl-Cq), 155.8 (aryl-Cq), 155.6 (aryl-Cq), 142.3 (aryl-CH), 137.4 (aryl-CH), 136.5 (aryl-CH), 135.2 (aryl-Cq), 133.3 (aryl-Cq), 130.7 (aryl-CH), 130.4 (aryl-CH), 129.4 (aryl-CH), 129.2 (aryl-CH), 128.9 (aryl-Cq), 127.9 (aryl-Cq), 127.7 (aryl-CH), 127.6 (aryl-CH), 125.3 (aryl-Cq), 124.0 (aryl-CH), 123.5 (aryl-CH), 122.7 (aryl-CH), 121.7 (aryl-CH), 120.8 (aryl-CH), 114.7 (aryl-Cq), 111.5 (aryl-CH), 54.9 (CH₃). Anal. Calcd for C₄₄H₃₃NO₂Si: C, 82.02; H, 5.33; N, 2.39. Found: C, 82.06; H, 5.40; N, 2.29.

Proligand e. A solution of 6-(2-hydroxy-3-(triphenylsilyl)naphthalen-1-yl)picolinaldehyde (1.20 g, 2.36 mmol) and 2,6-diisopropylaniline (0.54 g, 3.07 mmol) in THF (50 mL) containing 3 Å molecular sieves and a catalytic amount of TsOH was heated to reflux under argon for 12 h. After filtration and removal of the volatiles under vacuum, the crude material was recrystallized from a CH₂Cl₂/pentane mixture (1:1) to afford **e** as a microcrystalline yellow solid (1.20 g, 76%). ¹H NMR (400 MHz, CDCl₃, 298 K): δ 11.86 (br s, 1H, OH), 8.19 (s, 1H, CH=N), 8.15–8.12 (m, 1H, aryl-CH), 8.05 (d, $^3J_{H-H} = 8.5$, 1H, aryl-CH), 7.92–7.91 (m, 2H, aryl-CH), 7.73 (s, 1H, aryl-CH), 7.59–7.55 (m, 6H, aryl-CH), 7.31–7.18 (m, 12H, aryl-CH), 7.07–7.03 (m, 3H, aryl-CH), 2.87–2.84 (sept, $^3J_{H-H} = 7.4$, 2H, CH(CH₃)₂), 1.07 (d, $^3J_{H-H} = 7.4$, 12H, CH(CH₃)₂). ¹³C NMR (100 MHz, CDCl₃, 298 K): δ 161.8 (CH=N), 159.4 (aryl-Cq), 156.9 (aryl-Cq), 152.7 (aryl-Cq), 148.3 (aryl-Cq), 142.9 (aryl-CH), 137.8 (aryl-CH), 137.1 (aryl-Cq), 136.6 (aryl-CH), 136.5 (aryl-CH), 134.7 (aryl-Cq), 133.2 (aryl-Cq), 129.5 (aryl-CH), 129.4 (aryl-CH), 127.9 (aryl-CH), 127.7 (aryl-CH), 125.1 (aryl-Cq), 124.7 (aryl-CH), 123.3 (aryl-CH), 123.2 (aryl-CH), 119.5 (aryl-CH), 113.9

(aryl-Cq), 28.0 (CH(CH₃)₂), 22.4 (CH(CH₃)₂). Anal. Calcd for C₄₆H₄₂N₂OSi: C, 82.84; H, 6.35; N, 4.20. Found: C, 82.80; H, 6.39; N, 4.27.

Proligand f. To a solution of **e** (1.00 g, 1.49 mmol) in anhydrous, degassed Et₂O (5 mL) cooled to -30 °C under argon was added phenyllithium (2.25 mL of a 2 M solution in dibutyl ether, 4.49 mmol). After warming to room temperature, the reaction mixture was stirred for 12 h. The reaction was then quenched with aqueous NH₄Cl. The product was extracted with Et₂O (3 × 20 mL), and the combined organic extracts were dried over MgSO₄ and evaporated to afford **f** as a microcrystalline yellow solid (1.00 g, 90%). ¹H NMR (500 MHz, CDCl₃, 298 K): δ 11.66 (br s, 1H, OH), 8.17 (d, ³J_{H-H} = 8.5, 1H, aryl-CH), 7.88 (s, 1H, aryl-CH), 7.79 (d, ³J_{H-H} = 4.2, 2H, aryl-CH), 7.71–7.68 (m, 7H, aryl-CH), 7.67–7.65 (m, 1H, aryl-CH), 7.50–7.46 (m, 5H, aryl-CH), 7.43–7.39 (m, 6H, aryl-CH), 7.33–7.31 (m, 2H, aryl-CH), 7.23–7.20 (m, 3H, aryl-CH), 7.05–7.02 (m, 3H, aryl-CH), 5.24 (s, 1H, CHPh), 2.95–2.90 (sept, ³J_{H-H} = 6.8, 2H, CH(CH₃)₂), 1.05 (d, ³J_{H-H} = 6.8, 6H, CH(CH₃)₂), 1.02 (d, ³J_{H-H} = 6.7, 6H, CH(CH₃)₂). ¹³C NMR (125 MHz, CDCl₃, 298 K): δ 161.1 (aryl-Cq), 159.7 (aryl-Cq), 156.7 (aryl-Cq), 142.4 (aryl-CH), 142.1 (aryl-Cq), 141.9 (aryl-Cq), 141.1 (aryl-Cq), 137.4 (aryl-CH), 136.6 (aryl-CH), 134.8 (aryl-Cq), 133.1 (aryl-Cq), 129.4 (aryl-CH), 129.2 (aryl-CH), 128.9 (aryl-CH), 128.7 (aryl-CH), 128.6 (aryl-CH), 128.5 (aryl-CH), 127.6 (aryl-CH), 127.4 (aryl-CH), 127.2 (aryl-CH), 127.1 (aryl-CH), 126.1 (aryl-Cq), 125.4 (aryl-Cq), 124.5 (aryl-CH), 123.7 (aryl-CH), 123.6 (aryl-CH), 123.3 (aryl-CH), 122.8 (aryl-CH), 119.9 (aryl-CH), 113.9 (aryl-Cq), 69.6 (CHPh), 27.7 (CH(CH₃)₂), 24.1 (CH(CH₃)₂), 24.0 (CH(CH₃)₂). Anal. Calcd for C₅₂H₄₈N₂OSi: C, 83.83; H, 6.49; N, 3.76. Found: C, 83.90; H, 6.45; N, 3.71.

Complex 1a. A Schlenk flask was charged with proligand **a** (0.100 g, 0.112 mmol) and dried toluene (*ca.* 10 mL) was transferred in. ZnEt₂ (0.12 mL of a 1.0 M solution in toluene, 0.12 mmol) was added to the reaction mixture at -78 °C. The reaction mixture was gently warmed to room temperature and stirred 12 h. The solution was filtered, evaporated,

and the residue was washed with pentane and dried under vacuum to give **1a** as a yellow microcrystalline material (0.100 g, 90%). ^1H NMR (500 MHz, toluene- d_8 , 253 K): δ 8.31 (s, 1H, aryl-CH), 8.07 (s, 1H, aryl-CH), 7.96–7.94 (m, 6H, aryl-CH), 7.91 (d, $^3J_{\text{H-H}} = 8.5$, 1H, aryl-CH), 7.79 (d, $^3J_{\text{H-H}} = 8.3$, 1H, aryl-CH), 7.74 (d, $^3J_{\text{H-H}} = 7.2$, 6H, aryl-CH), 7.37 (d, $^3J_{\text{H-H}} = 8.1$, 1H, aryl-CH), 7.33 (d, $^3J_{\text{H-H}} = 7.9$, 1H, aryl-CH), 7.26 (d, $^3J_{\text{H-H}} = 8.1$, 1H, aryl-CH), 7.22–7.16 (m, 14H, aryl-CH), 7.05 (t, $^3J_{\text{H-H}} = 7.6$, 8H, aryl-CH), 6.77 (t, $^3J_{\text{H-H}} = 7.9$, 1H, aryl-CH), 6.45 (d, $^3J_{\text{H-H}} = 7.5$, 1H, aryl-CH), 2.34 (s, 3H, OCH₃), 0.45 (t, $^3J_{\text{H-H}} = 8.1$, 3H, ZnCH₂CH₃), -0.06–0.14 (m, 1H, ZnCH₂CH₃), -0.53–0.46 (m, 1H, ZnCH₂CH₃). $^{13}\text{C}\{^1\text{H}\}$ NMR (125 MHz, toluene- d_8 , 298 K): δ 169.3 (aryl-Cq), 158.1 (aryl-Cq), 143.8 (aryl-CH), 142.2 (aryl-CH), 137.0 (aryl-CH), 136.8 (aryl-CH), 130.1 (aryl-CH), 129.5 (aryl-CH), 129.2 (aryl-CH), 128.9 (aryl-CH), 128.8 (aryl-CH), 128.1 (aryl-CH), 128.0 (aryl-CH), 127.7 (aryl-CH), 127.2 (aryl-CH), 127.0 (aryl-CH), 125.7 (aryl-CH), 124.5 (aryl-CH), 124.2 (aryl-CH), 122.7 (aryl-CH), 121.1 (aryl-CH), 113.7 (aryl-CH), 59.2 (OCH₃), 11.8 (ZnCH₂CH₃), -1.8 (ZnCH₂CH₃). Anal. Calcd for C₆₄H₅₁NO₂Si₂Zn: C, 77.83; H, 5.20; N, 1.42. Found: C, 77.95; H, 5.02; N, 1.53. Yellow crystals of **1a** suitable for X-ray diffraction analysis were obtained by prolonged crystallization from a C₇H₈/heptane mixture (1:1) at room temperature.

Complex 1c. Using a procedure similar to that described above for **1a**, compound **1c** was obtained from **c** (0.100 g, 0.157 mmol) and ZnEt₂ (0.17 mL of a 1.0 M solution in toluene, 0.17 mmol) and isolated as a yellow microcrystalline material (0.111 g, 97%). ^1H NMR (500 MHz, THF- d_8 , 298 K): δ 7.95–7.91 (m, 2H, aryl-CH), 7.80–7.74 (m, 4H, aryl-CH), 7.71 (s, 1H, aryl-CH), 7.63 (d, $^3J_{\text{H-H}} = 7.1$, 6H, aryl-CH), 7.54 (d, $^3J_{\text{H-H}} = 7.8$, 1H, aryl-CH), 7.46–7.44 (m, 2H, aryl-CH), 7.37 (s, 1H, aryl-CH), 7.33–7.32 (m, 1H, aryl-CH), 7.26–7.21 (m, 10H, aryl-CH), 6.98 (t, $^3J_{\text{H-H}} = 7.4$, 1H, aryl-CH), 3.90 (s, 3H, OCH₃), 0.52 (t, $^3J_{\text{H-H}} = 8.0$, 3H, ZnCH₂CH₃), -0.61 (q, $^3J_{\text{H-H}} = 8.0$, 2H, ZnCH₂CH₃). ^{13}C NMR (125 MHz, THF- d_8 , 298 K): δ 170.8 (aryl-Cq), 159.6 (aryl-Cq), 156.9 (aryl-Cq), 155.7 (aryl-Cq), 143.3 (aryl-CH), 138.0 (aryl-CH), 137.6 (aryl-Cq), 137.4 (aryl-CH), 137.3 (aryl-CH), 136.9 (aryl-

Cq), 136.1 (aryl-Cq), 132.9 (aryl-CH), 131.8 (aryl-Cq), 130.7 (aryl-Cq), 129.7 (aryl-CH), 129.6 (aryl-Cq), 129.5 (aryl-Cq), 129.2 (aryl-CH), 128.9 (aryl-CH), 128.4 (aryl-CH), 128.1 (aryl-CH), 128.0 (aryl-CH), 127.9 (aryl-CH), 127.8 (aryl-Cq), 127.4 (aryl-CH), 127.3 (aryl-CH), 126.0 (aryl-Cq), 124.9 (aryl-CH), 124.2 (aryl-CH), 122.9 (aryl-CH), 120.8 (aryl-CH), 114.3 (aryl-Cq), 106.9 (aryl-CH), 55.85 (OCH₃), 12.75 (ZnCH₂CH₃), -1.15 (ZnCH₂CH₃). Anal. Calcd for C₄₆H₃₇NO₂SiZn: C, 75.76; H, 5.11; N, 1.92. Found: C, 75.63; H, 5.13; N, 1.95. Yellow crystals of **1c** suitable for X-ray diffraction analysis were obtained by prolonged crystallization from a THF/hexane mixture (1:1) at room temperature.

Complex 1d. Using a procedure similar to that described above for **1a**, compound **1d** was obtained from proligand **d** (0.100 g, 0.170 mmol) and ZnEt₂ (0.19 mL of a 1.0 M solution in toluene, 0.19 mmol) and isolated as a yellow microcrystalline material (0.080 g, 69%). ¹H NMR (500 MHz, C₆D₆, 298 K): δ 8.11 (s, 1H, aryl-CH), 7.98–7.96 (m, 6H, aryl-CH), 7.86 (d, ³J_{H-H} = 8.5, 1H, aryl-CH), 7.44 (d, ³J_{H-H} = 8.2, 1H, aryl-CH), 7.36 (d, ³J_{H-H} = 8.0, 1H, aryl-CH), 7.21–7.20 (m, 8H, aryl-CH), 7.17 (d, ³J_{H-H} = 7.9, 1H, aryl-CH), 7.09 (d, ³J_{H-H} = 7.3, 1H, aryl-CH), 7.02 (d, ³J_{H-H} = 7.6, 1H, aryl-CH), 6.98 (d, ³J_{H-H} = 7.1, 1H, aryl-CH), 6.93 (d, ³J_{H-H} = 7.9, 1H, aryl-CH), 6.85 (t, ³J_{H-H} = 7.9, 1H, aryl-CH), 6.75 (t, ³J_{H-H} = 7.4, 1H, aryl-CH), 6.50 (d, ³J_{H-H} = 7.6, 1H, aryl-CH), 6.40 (d, ³J_{H-H} = 8.3, 1H, aryl-CH), 3.12 (s, 3H, OCH₃), 0.78 (t, ³J_{H-H} = 8.1, 3H, ZnCH₂CH₃), 0.02 (s, 2H, ZnCH₂CH₃). ¹³C NMR (125 MHz, C₆D₆, 298 K): δ 170.2 (aryl-Cq), 156.9 (aryl-Cq), 155.4 (aryl-Cq), 153.9 (aryl-Cq), 144.5 (aryl-CH), 138.2 (aryl-CH), 137.2 (aryl-Cq), 137.1 (aryl-CH), 136.2 (aryl-Cq), 132.5 (aryl-Cq), 131.3 (aryl-CH), 130.8 (aryl-CH), 129.9 (aryl-CH), 129.3 (aryl-Cq), 129.1 (aryl-CH), 128.6 (aryl-Cq), 128.3 (aryl-CH), 128.2 (aryl-Cq), 127.9 (aryl-CH), 127.4 (aryl-CH), 126.9 (aryl-CH), 125.7 (aryl-Cq), 123.3 (aryl-CH), 123.0 (aryl-CH), 121.8 (aryl-CH), 121.5 (aryl-CH), 114.2 (aryl-Cq), 113.6 (aryl-CH), 56.4 (OCH₃), 12.3 (ZnCH₂CH₃), -2.44 (ZnCH₂CH₃). Anal. Calcd for C₄₂H₃₅NO₂SiZn: C, 74.27; H, 5.19; N, 2.06. Found: C, 74.51;

H, 5.22; N, 2.13. Yellow crystals of **1d** suitable for X-ray diffraction analysis were obtained by prolonged crystallization from a C₆H₆/hexane mixture (1:1) at room temperature.

Complex 2c. Using a procedure similar to that described above for **1a**, compound **2c** was obtained from proligand **c** (0.100 g, 0.157 mmol) and Zn[N(SiMe₃)₂]₂ (0.067 g, 0.173 mmol) and isolated as a yellow microcrystalline material (0.110 g, 81%). ¹H NMR (500 MHz, C₆D₆, 298 K): δ 8.09 (s, 1H, aryl-CH), 7.98 (d, ³J_{H-H} = 7.4, 1H, aryl-CH), 7.93 (d, ³J_{H-H} = 7.5, 6H, aryl-CH), 7.72 (s, 1H, aryl-CH), 7.55 (d, ³J_{H-H} = 8.0, 1H, aryl-CH), 7.52 (d, ³J_{H-H} = 8.3, 1H, aryl-CH), 7.48 (d, ³J_{H-H} = 8.1, 1H, aryl-CH), 7.32 (d, ³J_{H-H} = 8.0, 1H, aryl-CH), 7.23–7.20 (m, 12H, aryl-CH), 6.97 (t, ³J_{H-H} = 7.4, 2H, aryl-CH), 6.89 (t, ³J_{H-H} = 7.9, 1H, aryl-CH), 6.64 (t, ³J_{H-H} = 7.6, 1H, aryl-CH), 3.15 (s, 3H, OCH₃), 0.14 (s, 18H, ZnN(SiMe₃)₂). ¹³C NMR (125 MHz, C₆D₆, 298 K): δ 171.5 (aryl-Cq), 158.0 (aryl-Cq), 153.1 (aryl-Cq), 152.8 (aryl-Cq), 144.9 (aryl-CH), 138.1 (aryl-CH), 137.1 (aryl-CH), 136.9 (aryl-Cq), 136.3 (aryl-Cq), 134.8 (aryl-Cq), 131.8 (aryl-Cq), 131.4 (aryl-CH), 131.3 (aryl-Cq), 129.7 (aryl-CH), 129.4 (aryl-Cq), 129.3 (aryl-Cq), 129.2 (aryl-CH), 128.6 (aryl-Cq), 128.5 (aryl-CH), 128.3 (aryl-CH), 128.2 (aryl-CH), 128.1 (aryl-CH), 127.7 (aryl-CH), 127.6 (aryl-CH), 127.3 (aryl-CH), 126.6 (aryl-CH), 125.7 (aryl-Cq), 121.9 (aryl-CH), 121.8 (aryl-CH), 117.5 (aryl-CH), 113.0 (aryl-Cq), 61.4 (OCH₃), 5.4 (ZnN(SiMe₃)₂). Anal. Calcd for C₅₀H₅₀N₂O₂Si₃Zn: C, 69.78; H, 5.86; N, 3.26. Found: C, 69.86; H, 5.91; N, 3.21. Yellow crystals of **2c** suitable for X-ray diffraction analysis were prepared by prolonged crystallization from a toluene/hexane mixture (1:1) at room temperature.

Complex 2d. Using a procedure similar to that described above for **1a**, compound **2d** was obtained from proligand **d** (0.100 g, 0.170 mmol) and Zn[N(SiMe₃)₂]₂ (0.072 g, 0.187 mmol) and isolated as a yellow microcrystalline material (0.099 g, 72%). ¹H NMR (500 MHz, C₆D₆, 298 K): δ 8.11 (s, 1H, aryl-CH), 7.98 (d, ³J_{H-H} = 8.6, 1H, aryl-CH), 7.94 (d, ³J_{H-H} = 5.5, 6H, aryl-CH), 7.49 (d, ³J_{H-H} = 8.1, 1H, aryl-CH), 7.35 (d, ³J_{H-H} = 7.9, 1H, aryl-CH), 7.25–7.23 (m, 10H, aryl-CH), 7.17 (s, 1H, aryl-CH), 7.01–6.97 (m, 2H, aryl-CH), 6.89–6.85

(m, 2H, aryl-CH), 6.73 (d, $^3J_{H-H} = 8.0$, 1H, aryl-CH), 6.56 (d, $^3J_{H-H} = 7.5$, 1H, aryl-CH), 3.04 (s, 3H, OCH₃), -0.04 (s, 18H, ZnN(SiMe₃)₂). ¹³C NMR (125 MHz, C₆D₆, 298 K): δ 171.4 (aryl-Cq), 157.9 (aryl-Cq), 155.4 (aryl-Cq), 152.5 (aryl-Cq), 144.9 (aryl-CH), 138.0 (aryl-Cq), 137.1 (aryl-CH), 136.9 (aryl-Cq), 136.3 (aryl-Cq), 131.8 (aryl-Cq), 131.5 (aryl-CH), 130.7 (aryl-CH), 129.9 (aryl-Cq), 129.6 (aryl-CH), 129.1 (aryl-CH), 128.3 (aryl-CH), 128.1 (aryl-Cq), 128.0 (aryl-CH), 127.9 (aryl-Cq), 126.6 (aryl-CH), 126.5 (aryl-CH), 126.1 (aryl-CH), 123.4 (aryl-CH), 121.8 (aryl-CH), 121.3 (aryl-CH), 121.1 (aryl-CH), 113.0 (aryl-Cq), 61.5 (OCH₃), 5.49 (ZnN(SiMe₃)₂). Anal. Calcd for C₄₆H₄₈N₂O₂Si₃Zn: C, 68.16; H, 5.97; N, 3.46. Found: C, 68.09; H, 5.91; N, 3.52.

Complex 2e. Using a procedure similar to that described above for **1a**, compound **2e** was obtained from proligand **e** (0.100 g, 0.149 mmol) and Zn[N(SiMe₃)₂]₂ (0.069 g, 0.178 mmol) and isolated as a yellow microcrystalline solid (0.105 g, 79%). ¹H NMR (500 MHz, C₆D₆, 298 K): δ 8.08 (s, 1H, aryl-CH), 8.04 (d, $^3J_{H-H} = 8.2$, 1H, aryl-CH), 7.86–7.84 (m, 6H, aryl-CH), 7.67 (s, 1H, CH=N), 7.64 (d, $^3J_{H-H} = 8.4$, 1H, aryl-CH), 7.32–7.28 (m, 2H, aryl-CH), 7.19–7.18 (m, 8H, aryl-CH), 7.07 (t, $^3J_{H-H} = 7.5$, 1H, aryl-CH), 7.01–6.99 (m, 2H, aryl-CH), 6.68 (t, $^3J_{H-H} = 7.8$, 1H, aryl-CH), 6.22 (d, $^3J_{H-H} = 7.1$, 1H, aryl-CH), 3.15 (br s, 3H, CH(CH₃)₂), 2.95 (br s, 1H, CH(CH₃)₂), 1.39 (br s, 3H, CH(CH₃)₂), 1.12 (br s, 3H, CH(CH₃)₂), 1.04 (br s, 3H, CH(CH₃)₂), 0.87 (br s, 3H, CH(CH₃)₂), -0.13 (s, 18H, ZnN(SiMe₃)₂). ¹³C NMR (125 MHz, C₆D₆, 298 K): δ 173.2 (aryl-Cq), 162.5 (CH=N), 157.7 (aryl-Cq), 146.4 (aryl-CH), 143.9 (aryl-Cq), 143.3 (aryl-Cq), 137.3 (aryl-CH), 136.7 (aryl-CH), 136.4 (aryl-Cq), 134.8 (aryl-Cq), 132.2 (aryl-Cq), 130.9 (aryl-CH), 129.4 (aryl-CH), 128.8 (aryl-CH), 128.2 (aryl-Cq), 127.9 (aryl-CH), 127.8 (aryl-Cq), 127.7 (aryl-CH), 127.6 (aryl-CH), 127.5 (aryl-CH), 127.2 (aryl-Cq), 122.5 (aryl-CH), 121.8 (aryl-CH), 121.7 (aryl-CH), 112.8 (aryl-Cq), 28.9 (CH(CH₃)₂), 27.5 (CH(CH₃)₂), 26.1 (CH(CH₃)₂), 24.8 (CH(CH₃)₂), 23.8 (CH(CH₃)₂), 20.9 (CH(CH₃)₂), 4.86 (ZnN(SiMe₃)₂). Anal. Calcd for C₅₂H₅₉N₃OSi₃Zn: C, 70.04; H, 6.67; N, 4.71. Found: C, 69.92; H, 6.69; N, 4.79.

Complex 3c. Using a procedure similar to that described above for **1a**, compound **3c** was obtained from proligand **c** (0.100 g, 0.157 mmol) and AlMe_3 (0.17 mL of a 1.0 M solution in toluene, 0.17 mmol) and isolated as a yellow microcrystalline material (0.096 g, 88%). ^1H NMR (500 MHz, C_6D_6 , 298 K): δ 8.31 (s, 1H, aryl-CH), 7.92–7.90 (m, 6H, aryl-CH), 7.51 (d, $^3J_{\text{H-H}} = 8.3$, 2H, aryl-CH), 7.41 (d, $^3J_{\text{H-H}} = 8.0$, 2H, aryl-CH), 7.23 (q, $^3J_{\text{H-H}} = 7.4$, 2H, aryl-CH), 7.14–7.12 (m, 8H, aryl-CH), 7.09–7.06 (m, 4H, aryl-CH), 6.98 (d, $^3J_{\text{H-H}} = 7.7$, 1H, aryl-CH), 6.85 (br s, 1H, aryl-CH), 3.23 (s, 3H, OCH_3), -0.91 (s, 3H, $\text{Al}(\text{CH}_3)_2$), -1.33 (s, 3H, $\text{Al}(\text{CH}_3)_2$). ^{13}C NMR (125 MHz, C_6D_6 , 298 K): δ 164.3 (aryl-Cq), 156.6 (aryl-Cq), 155.7 (aryl-Cq), 154.2 (aryl-Cq), 144.2 (aryl-CH), 137.0 (aryl-CH), 136.9 (aryl-CH), 136.7 (aryl-CH), 135.4 (aryl-Cq), 135.2 (aryl-Cq), 134.2 (aryl-Cq), 130.1 (aryl-Cq), 129.9 (aryl-CH), 129.1 (aryl-CH), 129.0 (aryl-Cq), 128.9 (aryl-CH), 128.3 (aryl-CH), 128.2 (aryl-CH), 128.1 (aryl-Cq), 128.0 (aryl-CH), 127.9 (aryl-Cq), 127.8 (aryl-CH), 127.7 (aryl-CH), 127.6 (aryl-Cq), 127.5 (aryl-CH), 127.2 (aryl-CH), 126.5 (aryl-CH), 125.3 (aryl-CH), 124.7 (aryl-CH), 122.5 (aryl-CH), 114.7 (aryl-Cq), 106.8 (aryl-CH), 55.0 (OCH_3), -9.7 (AlCH_3), -11.3 (AlCH_3). Anal. Calcd for $\text{C}_{46}\text{H}_{38}\text{AlNO}_2\text{Si}$: C, 79.86; H, 5.54; N, 2.02. Found: C, 79.89; H, 5.56; N, 2.15. Yellow crystals of **3c** suitable for X-ray analysis were obtained by prolonged crystallization from a THF/hexane mixture (1:1) at room temperature.

Reaction of proligand e with AlMe_3 . Synthesis of Complex 3e' and Isolation of X-ray Suitable Crystals of 3e''. A Schlenk flask was charged with proligand **e** (0.100 g, 0.149 mmol) and toluene (*ca.* 10 mL) was transferred in. AlMe_3 (0.16 mL of a 1.0 M solution in toluene, 0.165 mmol) was added to the reaction mixture at -78 °C. The reaction mixture was stirred at room temperature overnight. The solution was filtered and volatiles were evaporated under vacuum affording **3e'** as a pale yellow microcrystalline powder (0.098 g, 91%). ^1H NMR (500 MHz, C_6D_6 , 298 K): δ 8.19 (d, $^3J_{\text{H-H}} = 8.8$, 1H, aryl-CH), 8.09 (s, 1H, aryl-CH), 7.83–7.79 (m, 6H, aryl-CH), 7.46 (d, $^3J_{\text{H-H}} = 8.0$, 1H, aryl-CH), 7.32–7.29 (m, 2H, aryl-CH), 7.17–7.01 (m, 10H, aryl-CH), 7.06 (t, $^3J_{\text{H-H}} = 8.0$, 3H, aryl-CH), 6.87 (t, $^3J_{\text{H-H}} =$

8.0, 1H, aryl-CH), 6.44 (d, $^3J_{H-H} = 7.8$, 1H, aryl-CH), 4.81 (q, $^3J_{H-H} = 6.0$, 1H, CHCH₃), 3.70 (sept, $^3J_{H-H} = 6.6$, 1H, CH(CH₃)₂), 3.40 (sept, $^3J_{H-H} = 6.6$, 1H, CH(CH₃)₂), 1.36 (d, $^3J_{H-H} = 6.6$, 3H, CH(CH₃)₂), 1.21 (d, $^3J_{H-H} = 6.6$, 3H, CH(CH₃)₂), 1.20 (d, $^3J_{H-H} = 6.6$, 3H, CH(CH₃)₂), 1.03 (d, $^3J_{H-H} = 6.0$, 3H, CHCH₃), 0.58 (d, $^3J_{H-H} = 6.6$, 3H, CH(CH₃)₂), -0.85 (s, 3H, AlCH₃). ¹³C NMR (125 MHz, C₆D₆, 298 K): δ 165.4 (aryl-Cq), 163.9 (aryl-Cq), 152.7 (aryl-Cq), 148.5 (aryl-Cq), 146.6 (aryl-Cq), 145.3 (aryl-CH), 142.3 (aryl-Cq), 139.2 (aryl-CH), 136.7 (aryl-CH), 136.6 (aryl-CH), 135.4 (aryl-Cq), 133.5 (aryl-Cq), 131.0 (aryl-Cq), 129.7 (aryl-CH), 129.1 (aryl-CH), 128.8 (aryl-Cq), 127.7 (aryl-CH), 127.6 (aryl-CH), 124.4 (aryl-CH), 124.1 (aryl-CH), 123.4 (aryl-CH), 123.0 (aryl-CH), 122.7 (aryl-CH), 118.0 (aryl-CH), 114.9 (aryl-Cq), 61.2 (CHCH₃), 27.9 (CH(CH₃)₂), 27.3 (CH(CH₃)₂), 26.7 (CH(CH₃)₂), 25.3 (CH(CH₃)₂), 25.0 (CH(CH₃)₂), 22.5 (CH(CH₃)₂), 21.8 (CHCH₃), -14.2 (AlCH₃). Anal. Calcd for C₄₈H₄₇AlN₂OSi: C, 79.74; H, 6.55; N, 3.87. Found: C, 79.81; H, 6.50; N, 3.80. Recrystallization of **3e'** from a solution in a toluene/hexanes mixture at room temperature resulted in isolation of crystals of partial hydrolysis product **3e''**,

Complex 4e. A Schlenk flask was charged with proligand **e** (0.100 g, 0.149 mmol) and Y[N(SiHMe₂)₃THF] (0.084 g, 0.149 mmol), and toluene (*ca.* 10 mL) was vacuum transferred in. The reaction mixture was stirred for 12 h at room temperature, then filtered and evaporated under vacuum. The solid residue was washed with pentane (10 mL) and dried under vacuum to give **4e** as a red microcrystalline material (0.133 g, 87%). ¹H NMR (500 MHz, C₆D₆, 333 K): δ 8.08 (s, 1H, aryl-CH), 7.99 (s, 1H, CH=N), 7.91–7.90 (m, 6H, aryl-CH), 7.79 (d, $^3J_{H-H} = 7.7$, 1H, aryl-CH), 7.36 (d, $^3J_{H-H} = 8.0$, 1H, aryl-CH), 7.25–7.24 (m, 10H, aryl-CH), 7.12 (s, 2H, aryl-CH), 7.01–6.99 (m, 2H, aryl-CH), 6.89 (t, $^3J_{H-H} = 7.7$, 1H, aryl-CH), 6.53 (d, $^3J_{H-H} = 6.2$, 1H, aryl-CH), 4.67 (br s, 4H, N(SiHMe₂)₂), 3.16 (br s, 2H, CH(CH₃)₂), 1.39 (d, $^3J_{H-H} = 5.2$, 6H, CH(CH₃)₂), 1.04 (d, $^3J_{H-H} = 5.2$, 6H, CH(CH₃)₂), -0.09 (s, 12H, N(SiHMe₂)₂), -0.16 (s, 12H, N(SiHMe₂)₂). ¹³C NMR (125 MHz, C₆D₆, 333 K): δ 171.2 (CH=N), 168.9 (aryl-Cq), 159.1 (aryl-Cq), 147.8 (aryl-Cq), 147.3 (aryl-Cq), 146.4

(aryl-CH), 140.3 (aryl-Cq), 136.9 (aryl-CH), 136.7 (aryl-CH), 136.2 (aryl-Cq), 135.1 (aryl-Cq), 133.1 (aryl-CH), 129.3 (aryl-CH), 128.9 (aryl-CH), 128.8 (aryl-Cq), 127.9 (aryl-CH), 127.6 (aryl-CH), 127.1 (aryl-CH), 125.2 (aryl-Cq), 124.6 (aryl-CH), 124.1 (aryl-CH), 123.3 (aryl-CH), 121.9 (aryl-CH), 114.9 (aryl-Cq), 28.5 (CH(CH₃)₂), 26.2 (CH(CH₃)₂), 2.8 (N(SiHMe₂)₂), 2.2 (N(SiHMe₂)₂). ²⁹Si{¹H} NMR (79 MHz, C₆D₆, 333 K): δ -11.5 (s, 1Si, Ph₃Si), -22.7 (br s, 2Si, SiHMe₂), -22.8 (br s, 2Si, SiHMe₂). ²⁹Si NMR (79 MHz, C₆D₆, 333 K): δ -22.7 (d sept, ¹J_{Si-H} = 165, ²J_{Si-H} = 6.8, 2Si), -22.8 (d sept, ¹J_{Si-H} = 165, ²J_{Si-H} = 6.8, 2Si). Anal. Calcd for C₅₄H₆₉N₄OSi₅Y: C, 63.62; H, 6.82; N, 5.50. Found: C, 63.70; H, 6.89; N, 5.60.

Complex 4f. Using a procedure similar to that described above for **4e**, compound **4f** was obtained from proligand **f** (0.050 g, 0.067 mmol) and Sc[N(SiHMe₂)₂]₃THF (0.0345 g, 0.067 mmol). Compound **4f** was isolated as an orange microcrystalline material (0.045 g, 67%). ¹H NMR (500 MHz, C₆D₆, 298 K): δ 8.26 (d, ³J_{H-H} = 8.5, 1H, aryl-CH), 8.01 (s, 1H, aryl-CH), 7.87–7.85 (m, 2H, aryl-CH), 7.81–7.79 (m, 6H, aryl-CH), 7.63 (d, ³J_{H-H} = 7.2, 2H, aryl-CH), 7.53 (d, ³J_{H-H} = 7.9, 1H, aryl-CH), 7.45 (d, ³J_{H-H} = 7.5, 1H, aryl-CH), 7.34 (d, ³J_{H-H} = 8.0, 2H, aryl-CH), 7.19–7.15 (m, 9H, aryl-CH), 7.03–7.00 (m, 4H, aryl-CH), 6.83 (t, ³J_{H-H} = 7.8, 1H, aryl-CH), 6.55 (d, ³J_{H-H} = 7.6, 1H, aryl-CH), 5.58 (s, 1H, CHPh), 4.84 (sept, ³J_{H-H} = 3.0, 2H, N(SiHMe₂)₂), 3.85 (sept, ³J_{H-H} = 6.8, 1H, CH(CH₃)₂), 3.17–3.14 (m, 3H, α-CH₂, THF + CH(CH₃)₂), 3.01–2.99 (m, 2H, α-CH₂, THF), 1.47 (d, ³J_{H-H} = 6.8, 3H, CH(CH₃)₂), 1.22 (d, ³J_{H-H} = 6.8, 3H, CH(CH₃)₂), 1.01 (d, ³J_{H-H} = 6.8, 3H, CH(CH₃)₂), 0.71–0.67 (m, 4H, β-CH₂ THF), 0.43 (d, ³J_{H-H} = 6.8, 3H, CH(CH₃)₂), 0.07 (d, ³J_{H-H} = 3.0, 6H, N(SiHMe₂)₂), 0.05 (d, ³J_{H-H} = 3.0, 6H, N(SiHMe₂)₂). ¹³C NMR (125 MHz, C₆D₆, 298 K): δ 166.6 (aryl-Cq), 165.3 (aryl-Cq), 154.1 (aryl-Cq), 151.6 (aryl-Cq), 147.0 (aryl-Cq), 146.1 (aryl-Cq), 145.5 (aryl-Cq), 145.3 (aryl-CH), 141.4 (aryl-Cq), 141.1 (aryl-Cq), 136.8 (aryl-CH), 136.6 (aryl-CH), 136.5 (aryl-CH), 135.1 (aryl-Cq), 129.8 (aryl-CH), 129.1 (aryl-CH), 128.7 (aryl-CH), 128.3 (aryl-Cq), 128.1 (aryl-CH), 127.7 (aryl-CH), 127.6 (aryl-CH), 127.2 (aryl-CH), 127.1

(aryl-CH), 127.0 (aryl-CH), 126.9 (aryl-CH), 126.4 (aryl-Cq), 125.9 (aryl-Cq), 125.0 (aryl-CH), 124.4 (aryl-CH), 123.9 (aryl-CH), 123.7 (aryl-CH), 123.5 (aryl-CH), 121.9 (aryl-CH), 119.3 (aryl-CH), 117.3 (aryl-Cq), 79.2 (CHPh), 71.7 (α -CH₂, THF), 27.5 (CH(CH₃)₂), 27.1 (CH(CH₃)₂), 26.9 (CH(CH₃)₂), 25.2 (CH(CH₃)₂), 25.1 (CH(CH₃)₂), 25.0 (CH(CH₃)₂), 24.3 (β -CH₂, THF), 3.1 (N(SiHMe₂)₂), 3.0 (N(SiHMe₂)₂). ²⁹Si{¹H} NMR (79 MHz, C₆D₆, 298 K) (the signal from the Ph₃Si group was not observed): δ -21.4 (s, 2Si). ²⁹Si NMR (79 MHz, C₆D₆, 298 K): δ -21.3 (d m, ¹J_{Si-H} = 180, 2Si). Anal. Calcd for C₆₀H₆₇N₃O₂Si₃Sc: C, 72.69; H, 6.81; N, 4.24. Found: C, 72.61; H, 6.89; N, 4.30.

Complex 5f. A Schlenk flask was charged with proligand **f** (0.100 g, 0.134 mmol) and Y[N(SiHMe₂)₂]₃THF (0.075 g, 0.134 mmol), and toluene (*ca.* 10 mL) was vacuum transferred in. The reaction mixture was stirred 12 h at 50 °C, then filtered and evaporated under vacuum. The residue was washed with pentane (10 mL) and dried under vacuum to give **5f** as an orange microcrystalline material (0.110 g, 81%). ¹H NMR (400 MHz, toluene-*d*₈, 298 K): δ 8.09 (d, ³J_{H-H} = 8.6, 1H, aryl-CH), 7.93 (s, 1H, aryl-CH), 7.83–7.81 (m, 6H, aryl-CH), 7.70 (d, ³J_{H-H} = 7.1, 2H, aryl-CH), 7.45–7.40 (m, 2H, aryl-CH), 7.35 (d, ³J_{H-H} = 8.0, 1H, aryl-CH), 7.28–7.24 (m, 3H, aryl-CH), 7.23–7.21 (m, 7H, aryl-CH), 7.13–6.91 (m, 6H, aryl-CH), 6.71 (d, ³J_{H-H} = 7.1, 1H, aryl-CH), 5.34 (s, 1H, CHPh), 4.70 (sept, ³J_{H-H} = 3.0, 2H, N(SiHMe₂)₂), 3.77 (sept, ³J_{H-H} = 6.8, 1H, CH(CH₃)₂), 3.12 (sept, ³J_{H-H} = 6.8, 1H, CH(CH₃)₂), 2.87–2.83 (m, 2H, α -CH₂, THF), 2.75–2.71 (m, 2H, α -CH₂, THF), 1.42 (d, ³J_{H-H} = 6.8, 3H, CH(CH₃)₂), 1.18 (d, ³J_{H-H} = 6.8, 3H, CH(CH₃)₂), 1.02 (d, ³J_{H-H} = 6.8, 3H, CH(CH₃)₂), 0.74–0.71 (m, 4H, β -CH₂, THF), 0.49 (d, ³J_{H-H} = 6.8, 3H, CH(CH₃)₂), 0.18 (d, ³J_{H-H} = 3.0, 6H, N(SiHMe₂)₂), 0.11 (d, ³J_{H-H} = 3.0, 6H, N(SiHMe₂)₂). ¹³C NMR (100 MHz, toluene-*d*₈, 298 K): δ 168.0 (aryl-Cq), 164.8 (aryl-Cq), 155.8 (aryl-Cq), 152.5 (aryl-Cq), 147.8 (aryl-Cq), 147.2 (aryl-Cq), 146.6 (aryl-Cq), 145.2 (aryl-CH), 137.3 (aryl-Cq), 136.9 (aryl-CH), 136.7 (aryl-CH), 136.4 (aryl-Cq), 129.3 (aryl-CH), 129.2 (aryl-CH), 129.1 (aryl-CH), 128.9 (aryl-CH), 128.5 (aryl-CH), 128.0 (aryl-CH), 127.7 (aryl-Cq), 127.4 (aryl-CH), 127.2 (aryl-CH),

127.0 (aryl-CH), 126.2 (aryl-CH), 125.3 (aryl-Cq), 124.9 (aryl-CH), 124.3 (aryl-CH), 123.7 (aryl-CH), 123.0 (aryl-CH), 121.9 (aryl-CH), 119.8 (aryl-CH), 117.8 (aryl-Cq), 81.0 (CHPh), 70.8 (α -CH₂, THF), 27.9 (CH(CH₃)₂), 27.5 (CH(CH₃)₂), 26.6 (CH(CH₃)₂), 25.8 (CH(CH₃)₂), 25.6 (CH(CH₃)₂), 25.0 (CH(CH₃)₂), 24.7 (β -CH₂, THF), 3.7 (N(SiHMe₂)₂), 3.3 (N(SiHMe₂)₂).
²⁹Si{¹H} NMR (79 MHz, toluene-*d*₈, 298 K): δ -11.8 (s, 1Si, Ph₃Si), -21.9 (s, 2Si, SiHMe₂).
²⁹Si NMR (79 MHz, toluene-*d*₈, 298 K): δ -21.9 (d m, ¹J_{Si-H} = 165, 2Si). Anal. Calcd for C₆₀H₆₇N₃O₂Si₃Y: C, 69.60; H, 6.52; N, 4.06. Found: C, 69.85; H, 6.57; N, 4.11.

Complex 6f. Using a procedure similar to that described above for **5f**, compound **6f** was obtained from proligand **f** (0.100 g, 0.134 mmol) and La[N(SiHMe₂)₂]₃(THF)₂ (0.091 g, 0.134 mmol). Compound **6f** was isolated as an orange microcrystalline material (0.120 g, 83%). ¹H NMR (500 MHz, C₆D₆, 298 K): δ 7.99 (s, 1H, aryl-CH), 7.84–7.82 (m, 6H, aryl-CH), 7.74 (d, ³J_{H-H} = 7.1, 1H, aryl-CH), 7.46–7.44 (m, 1H, aryl-CH), 7.35 (d, ³J_{H-H} = 8.1, 1H, aryl-CH), 7.32 (d, ³J_{H-H} = 8.1, 1H, aryl-CH), 7.27 (t, ³J_{H-H} = 7.6 Hz, 3H, aryl-CH), 7.20–7.15 (m, 9H, aryl-CH), 7.07–7.01 (m, 5H, aryl-CH), 6.96–6.93 (m, 1H, aryl-CH), 6.86 (t, ³J_{H-H} = 7.6, 1H, aryl-CH), 6.69 (d, ³J_{H-H} = 7.6, 1H, aryl-CH), 5.40 (s, 1H, CHPh), 4.78 (br s, 2H, N(SiHMe₂)₂), 3.77 (sept, ³J_{H-H} = 6.5, 1H, CH(CH₃)₂), 3.03 (sept, ³J_{H-H} = 6.5, 1H, CH(CH₃)₂), 2.67 (br s, 4H, α -CH₂, THF), 1.31 (d, ³J_{H-H} = 6.5, 3H, CH(CH₃)₂), 1.21 (d, ³J_{H-H} = 6.5, 3H, CH(CH₃)₂), 0.93 (d, ³J_{H-H} = 6.5, 3H, CH(CH₃)₂), 0.83 (br s, 4H, β -CH₂, THF), 0.55 (d, ³J_{H-H} = 6.5, 3H, CH(CH₃)₂), 0.13 (d, ³J_{H-H} = 3.0, 6H, N(SiHMe₂)₂), 0.11 (d, ³J_{H-H} = 3.0, 6H, N(SiHMe₂)₂). ¹³C NMR (125 MHz, C₆D₆, 298 K): δ 168.4 (aryl-Cq), 162.8 (aryl-Cq), 155.2 (aryl-Cq), 148.6 (aryl-Cq), 148.4 (aryl-Cq), 147.8 (aryl-Cq), 147.2 (aryl-Cq), 144.4 (aryl-CH), 141.4 (aryl-Cq), 141.1 (aryl-Cq), 137.1 (aryl-Cq), 136.5 (aryl-CH), 129.0 (aryl-CH), 128.9 (aryl-Cq), 128.8 (aryl-CH), 128.7 (aryl-CH), 128.5 (aryl-CH), 128.4 (aryl-CH), 128.3 (aryl-CH), 127.8 (aryl-CH), 127.2 (aryl-CH), 127.1 (aryl-CH), 126.9 (aryl-CH), 126.6 (aryl-CH), 124.5 (aryl-CH), 124.3 (aryl-CH), 123.5 (aryl-CH), 122.9 (aryl-CH), 121.5 (aryl-CH), 119.6 (aryl-CH), 117.9 (aryl-Cq), 81.9 (CHPh), 68.9 (α -CH₂, THF), 27.5 (CH(CH₃)₂), 27.4

(CH(CH₃)₂), 26.1 (CH(CH₃)₂), 25.7 (CH(CH₃)₂), 25.6 (CH(CH₃)₂), 24.6 (β-CH₂, THF), 3.1 (N(SiHMe₂)₂), 0.2 (N(SiHMe₂)₂). ²⁹Si{¹H} NMR (79 MHz, C₆D₆, 298 K): δ -11.5 (s, 1Si, Ph₃Si), -24.7 (s, 2Si, SiHMe₂). ²⁹Si NMR (79 MHz, C₆D₆, 298 K): δ -24.7 (d sept, ¹J_{Si-H} = 163, ²J_{Si-H} = 6.6, 2Si). Anal. Calcd for C₆₀H₆₇N₃O₂Si₃La: C, 66.40; H, 6.22; N, 3.87. Found: C, 66.49; H, 6.19; N, 3.92.

General Procedure for Polymerization of *rac*-Lactide. In a typical experiment (Table 1, entry 5), in a glovebox, a Schlenk flask was charged with a solution of complex **1c** (10.0 mg, 13.7 μmol) in toluene (1.0 mL). To this solution, *rac*-lactide (0.197 g, 1.37 mmol, 100 equiv vs. Zn) was added rapidly. The mixture was immediately stirred with a magnetic stirrer bar at 80 °C for 30 min. Aliquots of the crude material were periodically sampled by pipette for determining the monomer conversion by ¹H NMR spectroscopy in CDCl₃, from the integration (Int.) ratio Int._{polymer}/[Int._{polymer}+Int._{monomer}], using the methyl hydrogen resonances for PLA at δ 1.49 ppm and for LA at δ 1.16 ppm. The reaction was quenched with a solution of H₂O in THF (ca. 1 mL, 10 wt-%), and the polymer was precipitated with an excess amount of methanol (ca. 100 mL). The polymer was then filtered and dried under vacuum to a constant weight. The microstructure of PLAs was determined by homodecoupling ¹H NMR spectroscopy (methine region) at 20 °C in CDCl₃ on a Bruker AC-500 spectrometer.

General Procedure for Polymerization of *rac*-β-Butyrolactone. In a typical experiment (Table 2, entry 2), in a glovebox, a Schlenk flask was charged with a solution of complex **2c** (10.0 mg, 11.6 μmol) in toluene (1.1 mL). To this solution, *rac*-β-butyrolactone (0.99 g, 1.16 mmol, 100 equiv vs. Zn) was added rapidly. The mixture was immediately stirred with a magnetic stirrer bar at 80 °C for 4.5 h. The reaction was processed and worked-up similarly to that described above for lactide polymerization. Monomer conversions were calculated from ¹H NMR spectra of the crude reaction mixtures in CDCl₃, from the integration (Int.) ratio Int._{polymer}/[Int._{polymer}+Int._{monomer}], using the methylene hydrogen

resonances for PHB at δ 1.49 ppm and for BBL at δ 1.16 ppm. The microstructure of PHBs was determined by ^{13}C NMR spectroscopy (methylene region) at 20 °C in CDCl_3 on a Bruker AC-500 spectrometer.

Crystal Structures Determination. Diffraction data for **a**, **b** $\cdot\text{CHCl}_3$, **c**, **d**, **e** $\cdot\text{C}_5\text{H}_{12}$ and complexes **1a** $\cdot 0.5\text{C}_7\text{H}_8$, **1c**, **1d** $\cdot 1.5\text{C}_6\text{H}_6$, **2c**, **2e**, **3c** $\cdot\text{C}_4\text{H}_8\text{O}$, **3e''** were collected at 100(2) K using a Bruker APEX CCD diffractometer with graphite-monochromatized MoK_α radiation ($\lambda = 0.71073 \text{ \AA}$). A combination of ω and ϕ scans was carried out to obtain at least a unique data set. The crystal structures were solved by direct methods, remaining atoms were located from difference Fourier synthesis followed by full-matrix least-squares refinement based on F2 (programs SIR97 and SHELXL-97)²² with the aid of the WINGX program.²³ In most cases, many hydrogen atoms could be found from the Fourier difference analysis. Other hydrogen atoms were placed at calculated positions and forced to ride on the attached atom. The hydrogen atom contributions were calculated but not refined. All non-hydrogen atoms were refined with anisotropic displacement parameters. The locations of the largest peaks in the final difference Fourier map calculation as well as the magnitude of the residual electron densities were of no chemical significance. Crystal data and details of data collection and structure refinement for proligands **a**, **b** $\cdot\text{CHCl}_3$, **c**, **d**, **e** $\cdot\text{C}_5\text{H}_{12}$ and complexes **1a** $\cdot 0.5\text{C}_7\text{H}_8$, **1c**, **1d** $\cdot 1.5\text{C}_6\text{H}_6$, **2c**, **2e**, **3c** $\cdot\text{C}_4\text{H}_8\text{O}$, **3e''** are summarized in Tables S2 and S3.

Acknowledgments. We thank the University of Rennes 1 and CNRS for partial support of this work. We thank S. Sinbandhit (University of Rennes 1) for his help in conducting some NMR experiments.

Supporting Information available. Electronic supplementary information (ESI) available: Representative ^1H and $^{13}\text{C}\{^1\text{H}\}$ NMR spectra and crystallographic details of the prepared proligands, complexes and polymers. CCDC 1020173, 1020174, 1020175, 1020176,

1020177, 1022410, 1020167, 1020168, 1020169, 1020170 and 1020171 contain the supplementary crystallographic data for compounds **a**, **b**·CHCl₃, **c**, **d**, **e**·C₅H₁₂ and complexes **1a**·0.5C₇H₈, **1c**, **1d**·1.5C₆H₆, **2c**, **2e**, **3c**·C₄H₈O, **3e**'', respectively. These data can be obtained free of charge from The Cambridge Crystallographic Data Centre via www.ccdc.cam.ac.uk/data_request/cif.

References and Notes

- ¹ (a) Thomas, C. M. *Chem. Soc. Rev.* **2010**, *39*, 165. (b) Stanford, M. J.; Dove, A. P. *Chem. Soc. Rev.* **2010**, *39*, 486. (c) Carpentier, J.-F. *Macromol. Rapid Commun.* **2010**, *31*, 1696. (d) Dijkstra, P. J.; Du, H.; Feijen, J. *Polym. Chem.* **2011**, *2*, 520.
- ² A particular case when two stereocontrol mechanisms are operational at the same time has been reported to result in gradient multiblock PLAs, see: Pilone, A.; Press, K.; Goldberg, I.; Kol, M.; Mazzeo, M.; Lamberti, M. *J. Am. Chem. Soc.* **2014**, *136*, 2940.
- ³ Kirillov, E.; Roisnel, T.; Razavi, A.; Carpentier, J.-F. *Organometallics* **2009**, *28*, 5036.
- ⁴ For leading references to the use of group 13 complexes based on closely related *N*- and/or *O*-based tridentate dianionic ligands in the ROP of lactide/cyclic carbonates, see: (a) Hild, F.; BreLOT, L.; Dagonne, S. *Organometallics* **2011**, *30*, 5457. (b) Hild, F.; Dagonne, S. *Organometallics* **2012**, *31*, 1189. (c) Hild, F.; Neehaul, N.; Bier, F.; Wirsum, M.; Gourlaouen, C.; Dagonne, S. *Organometallics* **2013**, *32*, 587.
- ⁵ (a) Grunova, E.; Kirillov, E.; Roisnel, T.; Carpentier, J.-F. *Dalton Trans.* **2010**, *39*, 6739. (b) Klitzke, J. S.; Roisnel, T.; Kirillov, E.; Casagrande Jr, O.; Carpentier, J.-F. *Organometallics* **2014**, *33*, 309. (c) Klitzke, J. S.; Roisnel, T.; Kirillov, E.; Casagrande Jr, O.; Carpentier, J.-F. *Organometallics* **2014**, in press; [dx.doi.org/10.1021/om401214q](https://doi.org/10.1021/om401214q).
- ⁶ Related ligand systems have been recently employed for the preparation of complexes of magnesium, calcium and aluminum, see: (a) Yi, W.; Ma, H. *Inorg. Chem.* **2013**, *52*,

11821. (b) Yi, W.; Ma, H. *Dalton Trans.* **2014**, *43*, 5200. (c) Gao, B.; Duan, R.; Pang, X.; Li, X.; Qu, Z.; Tang, Z.; Zhuang, X.; Chen, X. *Organometallics* **2013**, *32*, 5435.
- ⁷ Doyle, D. J.; Gibson, V. C.; White, A. J. P. *Dalton Trans.* **2007**, 358.
- ⁸ (a) Chisholm, M. H.; Gallucci, J. C.; Zhen, H.; Huffman, J. C. *Inorg. Chem.* **2001**, *40*, 5051. (b) Darensbourg, D. J.; Karroonnirun, O. *Inorg. Chem.* **2010**, *49*, 2360.
- ⁹ (a) Tay, B.-Y.; Wang, C.; Chia, S.-C.; Stubbs, L. P.; Wong, P.-K.; van Meurs, M. *Organometallics* **2011**, *30*, 6028. (b) Olson, J. A.; Boyd, R.; Quail, J. W.; Foley, S. R. *Organometallics* **2008**, *27*, 5333. (c) Nienkemper, K.; Kehr, G.; Kehr, S.; Frohlich, R.; Erker, G. *J. Organomet. Chem.* **2008**, *693*, 1572.
- ¹⁰ Shannon, R. D. *Acta Crystallogr., Sect. A* **1976**, *32*, 751.
- ¹¹ (a) Procopio, L. J.; Carroll, P. J.; Berry, D. H. *J. Am. Chem. Soc.* **1994**, *116*, 177. (b) Herrmann, W. A.; Munck, F. C.; Artus, G. R. J.; Runte, O.; Anwander, R. *Organometallics* **1997**, *16*, 682. (c) Herrmann, W. A.; Eppinger, J.; Spiegler, M.; Runte, O.; Anwander, R. *Organometallics* **1997**, *16*, 1813. (d) Klimpel, M. G.; Gorlitzer, H. W.; Tafipolsky, M.; Spiegler, M.; Scherer, W.; Anwander, R. *J. Organomet. Chem.* **2002**, *647*, 236. (e) Sarazin, Y.; Roscsa, D.; Poirier, V.; Roisnel, T.; Silvestru, A.; Maron, L.; Carpentier, J.-F. *Organometallics* **2010**, *29*, 6569. (f) Rad'kov, V.; Trifonov, A.; Roisnel, T.; Carpentier, J.-F.; Kirillov, E. *Eur. J. Inorg. Chem.* **2014**, in press; dx.doi.org/10.1002/ejic.201402362.
- ¹² Complexes **4f–5f** have two stereogenic centers (N, Ln) and also feature atropisomery (planes of the naphthoxy and pyridine moieties) and should, in principle, exist as diastereomeric mixtures. We suggest that the non-observation of diastereomers in the NMR spectra of these complexes is due to very rapid site-exchange of the THF and amide ligands.
- ¹³ Howard, R. H.; Alonso-Moreno, C.; Broomfield, L. M.; Hughes, D. L.; Wright, J. A.; Bochmann, M. *Dalton Trans.* **2009**, 8667.

- ¹⁴ Ay, S.; Ziegert, R. E.; Zhang, H.; Nieger, M.; Rissanen, K.; Fink, K.; Kubas, A.; Gschwind, R. M.; Brase, S. *J. Am. Chem. Soc.* **2010**, 12899.
- ¹⁵ Zhang, C.; Wang, Z.-X. *J. Organomet. Chem.* **2008**, 693, 3151.
- ¹⁶ Normand, M.; Dorcet, V.; Kirillov, E.; Carpentier, J.-F. *Organometallics* **2013**, 32, 1694.
- ¹⁷ Chapurina, Y.; Klitzke, J.; de L. Casagrande, O. Jr.; Awada, M.; Dorcet, V.; Kirillov, E.; Carpentier, J.-F. *Dalton Trans.* **2014**, *in press*; dx.doi.org/10.1039/C4DT01206B.
- ¹⁸ Bouyahyi, M.; Sarazin, Y.; Casagrande, O. L., Jr.; Carpentier, J.-F. *Appl. Organomet. Chem.* **2012**, 26, 681.
- ¹⁹ Eppinger, J.; Spiegler, M.; Hieringer, W.; Herrmann, W. A.; Anwender, R. *J. Am. Chem. Soc.* **2000**, 122, 3080.
- ²⁰ Bochmann, M.; Bwembya, G.; Webb, K. J. *Inorg. Synth.*, **1997**, 31, 19.
- ²¹ Kowalski, A.; Duda, A.; Penczek, S. *Macromolecules* **1998**, 31, 2114.
- ²² (a) Altomare, A.; Burla, M. C.; Camalli, M.; Cascarano, G.; Giacovazzo, C.; Guagliardi, A.; Moliterni, A. G. G.; Polidori, G.; Spagna, R. *J. Appl. Cryst.* **1999**, 32, 115. (b) Sheldrick, G. M. SHELXS-97, Program for the Determination of Crystal Structures, University of Goettingen (Germany), **1997**. (c) Sheldrick, G. M. SHELXL-97, Program for the Refinement of Crystal Structures, University of Goettingen (Germany), **1997**. (d) Sheldrick, G. M. *Acta Cryst.* **2008**, 64, 112.
- ²³ Farrugia, L. J. *J. Appl. Cryst.* **1999**, 32, 837.

Table 1. ROP of *racemic* lactide promoted by complexes **1a**, **1c**, **1d**, **2c**, **2d**, **2e**, **3c**, **3e'**, **4e** and **4–6f**.^a

Entry	Complex	[LA] ₀ /[M] /[iPrOH] ₀ ^a	Temp (°C)	Time _b (h)	Conv. _c (%)	$M_{n,theo}$ ^d (g·mol ⁻¹) (× 10 ³)	$M_{n,NMR}$ ^e (g·mol ⁻¹) (× 10 ³)	$M_{n,SEC}$ ^f (g·mol ⁻¹) (× 10 ³)	\bar{D}_M ^f	P_r ^g
1	1a	100:1:0	25	24	0	-	nd	-	-	-
2	1a	100:1:0	100	48	0	-	nd	-	-	-
3	1a	100:1:5	100	48	90	2.6	6.5	6.2	1.31	0.54
4	1a	1,000:1:5	100	144	23	6.6	9.6	9.9	1.33	0.56
5 ^h	1c	100:1:0	60	4	91	13.1	nd	42.3	2.12	0.75
6	1c	100:1:0	80	0.5	92	13.2	nd	20.8	1.70	0.65
7	1d	100:1:0	80	0.33	82	11.8	nd	21.2	1.56	0.66
8	2c	100:1:0	25	0.33	90	12.9	nd	11.7	1.68	0.72
9	2c	250:1:0	25	0.5	84	30.3	nd	27.7	1.91	0.73
10	2c	500:1:0	25	0.66	57	41.1	nd	40.1	1.88	0.76
11	2c	1,000:1:0	25	1	38	54.7	nd	58.8	1.92	0.74
12	2c	2,000:1:0	25	1.75	77	222.2	nd	216.5	2.04	0.73
13	2c	100:1:1	25	7	0	-	-	-	-	-
14	2c	1,000:1:1	100	0.13	45	64.8	nd	30.6	1.46	0.65
15	2d	100:1:0	25	0.5	36	5.2	5.7	5.4	1.32	0.75
16	2e	100:1:0	25	0.33	99	14.3	nd	13.8	1.11	0.71
17	2e	500:1:0	25	1.33	85	61.2	nd	54.5	1.11	0.72
18	2e	100:1:1	25	24	0	-	-	-	-	-
19	2e	500:1:1	25	24	0	-	-	-	-	-
20	3c	100:1:0	100	24	84	12.1	nd	29.9	1.54	0.50
21	3c	100:1:2	100	16	91	13.1	13.0	12.6	1.37	0.54
22	3e'	100:1:0	100	24	92	13.2	12.9	13.4	1.17	0.50
23	3e'	100:1:1	100	14	80	11.5	12.2	11.9	1.14	0.50
24	4e	100:1:0	25	0.17	99	14.3	nd	27.5	2.13	0.80
25 ^h	4e	100:1:0	25	0.17	99	14.3	nd	33.9	2.11	0.79
26	4e	500:1:0	25	0.5	96	69.2	nd	140.3	2.10	0.80
27	4e	100:1:2	25	0.08	>99	14.4	10.9	11.5	1.21	0.78
28	4e	500:1:2	25	0.25	92	66.3	nd	56.1	1.35	0.79

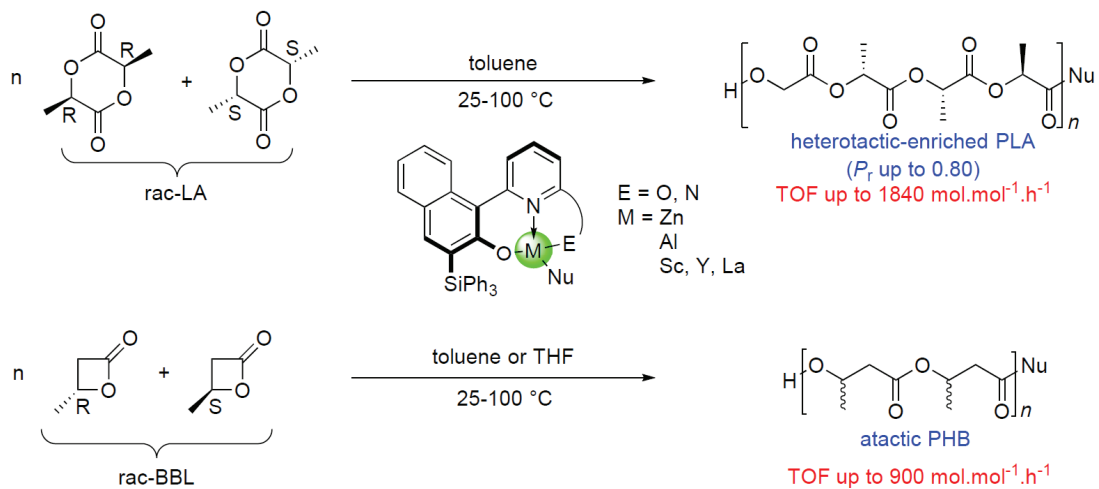
29	4f	100:1:0	60	1	68	9.8	11.6	11.0	1.47	0.58
30	5f	100:1:0	25	1.67	93	13.4	11.9	12.1	1.50	0.60
31 ^g	5f	100:1:0	25	1	83	11.9	nd	15.2	1.54	0.69
32	5f	500:1:0	25	6	44	31.7	nd	28.2	1.60	0.58
33	5f	100:1:1	25	0.83	98	14.1	16.4	15.8	1.43	0.57
34	6f	100:1:0	25	0.25	99	14.3	nd	14.2	1.98	0.69
35	6f	100:1:1	25	0.13	98	14.2	13.8	13.3	1.57	0.68

^a Polymerization conditions otherwise stated: $[rac-LA]_0 = 1.0$ M, solvent = toluene. ^b Reaction times were not necessarily optimized. ^c Monomer conversion determined by ¹H NMR spectroscopy (CDCl₃, 298 K). ^d Theoretical molecular weight calculated using $M_{n,theo} = conv(LA) \times [rac-LA]_0 / [M \text{ or } iPrOH] \times M_{LA}$. ^e Determined by ¹H NMR spectroscopy. ^f Experimental molecular weight determined by SEC vs. polystyrene standards and corrected by a factor of 0.58; $D_M = M_w/M_n$. ^g P_r is the probability of racemic linkage between monomer units, as determined from the methine region of the homonuclear decoupled ¹H NMR spectrum. ^h Carried out in THF.

Table 2. ROP of *racemic* β -butyrolactone promoted by complexes **2c**, **2e**, **3c**, **3e'**, **4e** and **4–6f**.^a

Entry	Complex	[BL] ₀ /[M] /[iPrOH] ₀ ^a	Temp (°C)	Time ^b (h)	Conv. ^c (%)	$M_{n,theo}$ ^d (g·mol ⁻¹) (× 10 ³)	$M_{n,SEC}$ ^e (g·mol ⁻¹) (× 10 ³)	\mathcal{D}_M ^e	P_r ^g
1	2c	100:1:0	25	24	0	-	-	-	-
2	2c	100:1:0	80	4.5	>99	8.6	19.2	1.22	nd
3	2c	500:1:0	60	14	70	30.1	39.3	1.07	0.56
4	2c	500:1:0	80	19	>99	43.0	55.9	1.07	0.56
5 ^h	2c	500:1:0	80	28	52	22.4	25.6	1.13	0.56
6	2e	100:1:0	60	4	85	7.3	15.2	1.23	0.50
7	3c	100:1:0	60	24	0	-	-	-	-
8	3c	100:1:2	100	24	0	-	-	-	-
9	3e'	100:1:0	100	24	0	-	-	-	-
10	4e	100:1:0	25	0.08	73	6.3	289.3 ^f	1.54 ^f	0.56
11	4f	100:1:0	60	24	0	-	-	-	-
12	5f	100:1:0	25	1	traces	nd	nd	nd	nd
13	5f	100:1:0	25	24	97	8.3	13.1	1.89	0.42
14	6f	100:1:0	25	24	81	6.9	11.1	1.48	0.66

^a All reactions performed with $[rac\text{-BL}]_0 = 1.0$ M. ^b Reaction times were not necessarily optimized. ^c BL conversion to PHB determined by ¹H NMR spectroscopy (CDCl₃, 298 K) on the crude reaction mixture. ^d Theoretical molecular weight calculated using $M_{n,theo} = \text{conv}(\text{BL}) \times [rac\text{-BL}]_0 / [M \text{ or } i\text{PrOH}] \times M_{BL}$. ^e Experimental (uncorrected) molecular weight determined by SEC in THF; $\mathcal{D}_M = M_w / M_n$. ^f Experimental (uncorrected) molecular weight determined by SEC in CHCl₃; $\mathcal{D}_M = M_w / M_n$. ^g P_r is the probability of racemic linkage between monomer units and is determined by ¹³C{¹H} NMR spectroscopy. ^h Carried out in THF.



ACCEPTED MANUSCRIPT

Highlights:

- New tridentate *ortho*-Ph₃Si-substituted naphthol-pyridine ligands were synthesized
- Zn, Al, Y and La complexes were prepared
- Some of these complexes exhibit high activity in ROP of lactide and β -butyrolactone
- Good molecular weight control and narrow distributions are achieved

ACCEPTED MANUSCRIPT